Earth Syst. Sci. Data, 14, 4757–4775, 2022
https://doi.org/10.5194/essd-14-4757-2022

Open Access Earth System Science Data

Multiyear emissions of carbonaceous aerosols from cooking, fireworks, sacrificial incense, joss paper burning, and barbecue as well as their key driving forces in China

Yi Cheng[1,2], Shaofei Kong[1,2], Liquan Yao[1,2], Huang Zheng[1,2], Jian Wu[1,2], Qin Yan[1,2], Shurui Zheng[1,2], Yao Hu[1,2], Zhenzhen Niu[1,2], Yingying Yan[1], Zhenxing Shen[3], Guofeng Shen[4], Dantong Liu[5], Shuxiao Wang[6], and Shihua Qi[2]

[1]Department of Atmospheric Science, School of Environmental Studies, China University of Geosciences, Wuhan, China
[2]Department of Environment Science and Engineering, School of Environmental Studies, China University of Geosciences, Wuhan, China
[3]Department of Environmental Science and Engineering, School of Energy and Power Engineering, Xi'an Jiaotong University, Xi'an, China
[4]Laboratory for Earth Surface Process, College of Urban and Environmental Sciences, Peking University, Beijing, China
[5]Department of Atmospheric Science, School of Earth Science, Zhejiang University, Hangzhou, China
[6]State Key Joint Laboratory of Environmental Simulation and Pollution Control, School of Environment, Tsinghua University, Beijing, China

Correspondence: Shaofei Kong (kongshaofei@cug.edu.cn)

Received: 8 May 2022 – Discussion started: 13 June 2022
Revised: 24 August 2022 – Accepted: 4 October 2022 – Published: 28 October 2022

Abstract. There has been controversy regarding the air pollutants emitted from sources closely related to the activities of daily life in China, such as cooking, setting off fireworks, sacrificial incense and joss paper burning, and barbecue (which have been named the five missing sources – FMSs), and the extent to which they impact the outdoor air quality. To date, due to the lack of both an activity dataset and emission factors, there have been no estimations of the emission of air pollutants from FMSs. In this work, we have attempted to combine questionnaire data, various statistical data, and data on points of interest to obtain a relatively complete set of activity data. The emission factors (EFs) of carbonaceous aerosols were tested in our lab. Emission inventories of carbonaceous aerosols with a high spatial–temporal resolution for FMSs were then established, and the spatial variation trend and driving forces were discussed. From 2000 to 2018, organic carbon (OC) emissions were in the range of 4268–4919 t. OC emissions from FMSs were between 1.5 ‰ and 2.2 ‰ of the total emissions in China. Black carbon (BC), elemental carbon (EC), and brown carbon (BrC) absorption cross-section (ACS_{BrC}) emissions from FMSs were in the ranges of 22.6–43.9 t, 213–324 t, and 14.7–35.6 Gm^2, respectively. Their emissions tended to be concentrated in certain periods and areas. The OC emission intensities in central urban areas were 3.85–50.5 times those in rural areas (due to the high density of human activity), while the ACS_{BrC} emissions in rural regions accounted for 63.0–79.5 % of the total emissions (resulting from uncontrolled fireworks). A mass of fireworks led to much higher ACS_{BrC} and EC emissions on Chinese New Year's Eve, with respective values that were 1444 and 262 times their corresponding yearly averages. Significant ($p<0.01$) correlations between the population's income and pollutant emissions were also found: these correlations were positive ($r = 0.94$) and negative ($r = -0.94$) for urban and rural regions, respectively, indicating the necessity to regulate residents' lifestyles and increase residents' income in respective urban and rural regions. This study

provides firsthand data to identify emissions, variation trends, and impacting factors from the FMSs. This is helpful for modeling works on air quality, the climate effect, and human health risks during specific periods or in specific regions as well as for modifying emission control policies. The data compiled in this work can found at https://doi.org/10.6084/m9.figshare.19999991.v2 (Cheng et al., 2022).

1 Introduction

China has experienced a period of serious air pollution, which has had serious health impacts on residents (Zheng et al., 2018; Q. Zhang et al., 2019; L. Zhang et al., 2020a; Tong et al., 2020). Carbonaceous aerosols (CAs), emitted from incomplete burning, include organic carbon (OC) and black carbon (BC) or elemental carbon (EC), and these species have attracted wide attention due to their adverse impacts on air quality, human health, and climate (Venkataraman et al., 2005; Ramanathan and Carmichael, 2008; Bond et al., 2013). The optical properties of CAs (especially brown carbon, BrC) are complex and mutative, which is also one of the important factors affecting the global radiation balance (Feng et al., 2013; Laskin et al., 2015).

Several sources closely related to traditional human activity are potential emission sources of CAs, such as the burning of sacrificial incense and joss paper, traditional Chinese barbecue, Chinese-style cooking, and fireworks. The estimation of air pollutant emissions from these sources has been omitted from existing emission inventories; thus, they have been defined as the "five missing sources" (FMSs) in this study. The FMSs can lead to a dramatic impact on the ambient air quality and human health over a short period or in a specific region (Chiang and Liao, 2006; Wu et al., 2015; Kong et al., 2015; Ho et al., 2016; Wang et al., 2017; Lai and Brimblecombe, 2020). For example, fireworks have been shown to contribute 60.1 % of $PM_{2.5}$ on Chinese New Year's Eve in Nanjing, and traditional sources such as sacrificial incense and joss paper burning could contribute 17.5 % of atmospheric polycyclic aromatic hydrocarbons (PAHs) in Chushan and 9.6 % of polychlorinated dibenzodioxins and furans (PCDD/F) in Taipei (Lin et al., 2008; Kong et al., 2015; Ho et al., 2016). Recently, due to the strengthened control of combustion-related sources, the important role of cooking emissions with respect to affecting air quality has gradually become visible in densely populated downtown areas. Cooking-related organic aerosol (COA) contributed 15 %–34 % of total OC emissions and 6 %–9 % of total $PM_{2.5}$ emissions in a downtown site in Shanghai (Huang et al., 2021) and 31 % of the total organic aerosol in Beijing in winter (Hu et al., 2021). Existing studies on the FMSs have mainly been based on ambient air monitoring datasets at certain sites or during certain periods (See and Balasubramanian, 2011; Wu et al., 2015; Shen et al., 2017; Lao et al., 2018; Tanda et al., 2019; Yao et al., 2019; Hu et al., 2021; Huang et al., 2021). However, to date, no studies have been able to provide their quantitative contributions on a large scale due to the scarcity of emission inventory information, which has limited the identification of their contributions in various regions or during certain periods. Questions also exist regarding whether or not the conclusions of prior studies are tenable, as they have been identified using models or ambient monitoring data, not using real emission estimation.

In China, the differences in population and economy between urban and rural areas are increasing (Meng et al., 2019), and the efficiency of and necessity for air quality control policies for the FMSs in urban and rural areas need to be assessed. For instance, fireworks are generally banned in central urban regions, whereas the suburbs and rural regions are less affected by such policies. Moreover, cooking smoke needs to be purified in city centers, whereas this policy may not be strictly executed or even necessary in suburban and rural areas. Such deviation in the establishment and implementation of policies could ultimately drive the differences in air pollutant emission distributions; however, these differences have not yet been addressed.

Emission inventories are the foundation of a quantitative description of anthropogenic pollutant emissions (Li et al., 2017). The combination of chemical transport models and high-resolution emission inventories has been paramount for understanding the impact of anthropogenic perturbations on the atmosphere and for assessing corresponding air pollution control strategies (Janssens-Maenhout et al., 2019; McDuffie et al., 2020). The lack of emission inventories has limited large-scale model simulations, the optimization of corresponding control measures, and the settlement of related disputes. In our previous work (Wu et al. 2021), we established an emission inventory of levoglucosan that included emissions from the FMSs (Wu et al., 2021). However, to the best of our knowledge, no other emission inventories of the FMSs have been reported.

In summary, this study aimed to develop a methodological framework for establishing an emission inventory of the FMSs, including methods for the acquisition of various activity data, emission factor monitoring, uncertainty assessment, and spatial–temporal allocation. The activity data were obtained based on household investigation, statistical data, and points of interest (POI), among other sources. The emission factors were monitored using a unique emission monitoring test platform, especially for fireworks, in our lab. A high spatial ($\sim$ 1 km) and temporal resolution (1 d for special festivals and 1 month for other periods) emission inventory was then established. The multiyear spatiotemporal variation in

CA emissions from these sources was analyzed and compared with other types of sources. Optimized pollution control measures were proposed for these types of sources. This work provides a methodology for establishing an emission inventory of air pollutants from sources closely related to human activity. Other air pollutant emissions could also be estimated in the future. The emission inventory obtained here could also provide basic input for corresponding modeling work.

2 Methodology

2.1 Combustion tests for emission factors

The combustion tests for the FMSs were performed using two custom-made combustion chambers: one of them had an explosion-proof function and was used in firework burning experiments, and the other was used in the sacrificial incense, joss paper, barbecue, and cooking emission experiments. A dilution sampling system (FPS-4000, Dekati, Finland) was employed to dilute the smoke. The smoke samples were diluted about 16–30 times and aged for about 30 s in a residence chamber. This sampling system has previously been utilized in residential fuel combustion experiments (Cheng et al., 2019; Yan et al., 2020; Y. Zhang et al., 2021; Wu et al., 2021). A total of 38 events were tested in this experiment: 6 trials of sacrificial incense combustion (including red incense – RI, environmental incense – EI, and high incense – HI), 6 trials of joss paper burning (including red-printed paper – RP, small sacrificial paper – SP, and large sacrificial paper – LP), 10 trials of fireworks (including firecrackers – FC, fountain fireworks – FF, handheld fireworks – HF, handheld fountain – HT, and spin fireworks – SF), 8 trials of barbecue (including chicken – CK, beef – BF, lamb – LB, and pork – PK), and 8 trials of cooking (including cooking of meat – MT1, cooking of meat and pepper – MT2, cooking of meat and garlic – MT3, and cooking of meat, pepper, and garlic – MT4). The materials used in the experiments are shown in Fig. S1.

After dilution, the OC and EC in the smoke samples were detected with an online CA analyzer developed by the Key Laboratory of Environmental Optics and Technology (Anhui Institute of Optics and Fine Mechanics, CAS) and based on the thermal–optical method (Ding et al., 2014). The analyzer showed reliable stability and repeatability. More details on the online CA analyzer can be found in Sect. S1. A dual-spot Aethalometer (Model AE33, Magee Scientific, USA) was employed to measure the BC concentration and particulate optical properties (Drinovec et al., 2015). The system used in the experiments is shown in Fig. S2.

2.2 Calculation of emission factors and optical properties

The emission factors (EF, mg kg $^{-1}$), of OC, EC, and BC were calculated as follows:

$$\mathrm{EF}_{ij} = \frac{v \times m_{ij} \times r}{v_0 \times M_j}, \tag{1}$$

where i and j denote the respective pollutant and material, v is the flue gas flow (L min^{-1}), v_0 is the sampling flow (L min^{-1}), m is the mass of the pollutant detected by the instruments (mg), r is the dilution ratio, and M is the mass of the material used in each trial (kg) (Cheng et al., 2019; Yan et al., 2020).

All filter-based optical measurements suffer from an underestimation caused by the loading effect (Drinovec et al., 2015); however, loading compensation can be calculated based on dual-spot measurements. The reader is referred to Drinovec et al. (2015) for the detailed calculation process. Inferior dependence of BC particles on light absorption at different light wavelengths has been found. The absorption Ångström exponent (AAE) is an exceptional parameter to describe this dependence, as shown in Eqs. (2) and (3):

$$b_{\mathrm{abs}} \sim \lambda^{-\mathrm{AAE}}, \tag{2}$$

$$\mathrm{AAE} = -\frac{\ln\left(\frac{b_{\mathrm{abs}}(\lambda_1)}{b_{\mathrm{abs}}(\lambda_2)}\right)}{\ln\left(\frac{\lambda_1}{\lambda_2}\right)}. \tag{3}$$

Here, λ is the wavelength, and b_{abs} denotes the total light absorption coefficient (Tian et al., 2019), which can be calculated as follows (Zotter et al., 2017):

$$\mathrm{BC} = b_{\mathrm{abs}}(\lambda)/\mathrm{MAC}(\lambda), \tag{4}$$

where MAC is the mass absorption cross-section, which is given by the Aethalometer manufacturer.

As shown in Eq. (5), the b_{abs} of CA was caused by BC and BrC. To calculate the $b_{\mathrm{abs}}(\lambda, \mathrm{BC})$ at each wavelength, Eq. (6) was introduced. The $\mathrm{AAE}_{\mathrm{BC}}$ was set as 1.0 according to previous studies (Tian et al., 2019; Liakakou et al., 2020). $f_{\mathrm{BrC}}(\lambda)$ (Eq. 7) was utilized to estimate the fraction of BrC light absorption ($b_{\mathrm{abs}}(\lambda, \mathrm{BrC})$) in total light absorption ($b_{\mathrm{abs}}(\lambda)$).

$$b_{\mathrm{abs}}(\lambda) = b_{\mathrm{abs}}(\lambda, \mathrm{BC}) + b_{\mathrm{abs}}(\lambda, \mathrm{BrC}) \tag{5}$$

$$b_{\mathrm{abs}}(\lambda, \mathrm{BC}) = b_{\mathrm{abs}}(880) \times \left(\frac{\lambda}{880}\right)^{-\mathrm{AAE}_{\mathrm{BC}}} \tag{6}$$

$$f_{\mathrm{BrC}}(\lambda) = 100\,\% \times b_{\mathrm{abs}}(\lambda, \mathrm{BrC})/b_{\mathrm{abs}}(\lambda) \tag{7}$$

Due to the complicated chemical properties of BrC, it was difficult to measure the accurate concentration of BrC in flue gases. Previous studies have developed a peculiar EF called the absorption emission factor (AEF), as shown in Eq. (8) (Martinsson et al., 2015; Tian et al., 2019; L. Zhang et al.,

2020b). Most studies have modeled the direct radiative forcing of BrC using its mass concentration and mass absorption efficiency (MAE) as the input parameters; however, the mass concentration and the total mass of BrC in the atmosphere are still unclear, and the MAE values (in the range of 0.08–3.8 $m^2\ g^{-1}$) are also variable (Park et al., 2010; Feng et al., 2013; X. Wang et al., 2014; A. Zhang et al., 2020). An inventory established using the AEF calculated with the following equation could avoid the deviation raised by the mass concentration and MAE of BrC (Tian et al., 2019):

$$\mathrm{AEF}_{ij} = \frac{\sum_{t_0}^{t_{\mathrm{sample}}} (b_{\mathrm{abs}_{ij}} \times r \times v)}{M_j}. \quad (8)$$

2.3 Acquisition of activity data

Data on the activity of sources directly affect the uncertainties in the emission inventory, and an accurate estimate of the FMSs' consumption was a crucial prerequisite. Statistics on the direct consumption of the FMSs are scarce. Thus, multiple activity data and proxy variables have been adopted in this work, including the statistical yearbooks of each province in China, datasets of POI (Sect. S2, Fig. S3), and rural household investigation data (Sect. S3).

The original information on the consumption of sacrificial incense, joss paper, and fireworks was obtained from household investigation; therefore, the information used was the per capita consumption of sacrificial incense, joss paper, and fireworks in each province. The data were adjusted to overcome the problem of insufficient sample size. In China, "sacrificial activity" refers to honoring ancestors, and it mainly takes place in temples or graveyards. China is a mountainous country with rolling terrain. Most of the inhabitants of non-plain areas chose hills that might be covered in vegetation as the site of graveyards. The data on the consumption of sacrificial incense and joss paper were revised based on the number of temples (from POI data) and the frequency of forest fires caused by sacrifices compared with the total frequency of forest fires (from China Forestry Statistical Yearbook data), as shown in Eq. (9):

$$\mathrm{Cs}_{\mathrm{adj,province}} = \mathrm{Cs}_{\mathrm{inv,province}} \times \left(\frac{\mathrm{Nt}_{\mathrm{province}}/\mathrm{POP}_{\mathrm{province}}}{2 \times \mathrm{Nt}_{\mathrm{nation}}/\mathrm{POP}_{\mathrm{nation}}} + \frac{\mathrm{Fs}_{\mathrm{province}}/\mathrm{Ft}_{\mathrm{province}}}{2 \times \mathrm{Fs}_{\mathrm{nation}}/\mathrm{Ft}_{\mathrm{nation}}} \right). \quad (9)$$

Here, Cs is the consumption of sacrificial incense or joss paper per capita; Nt is the number of temples; POP is the population, which was obtained from the statistical yearbook of each province; Fs is the frequency of forest fires caused by sacrificial activity; Ft is the frequency of forest fires caused by all anthropogenic activity; adj represents the data after adjustment; inv represents the data from the household investigation; province represents the data of each province; and nation represents the data of the entire nation.

The firework consumption amounts were revised based on the number of retail shops selling fireworks (from POI data) and the provincial fireworks export volume (statistical data), as shown in Eq. (10):

$$\mathrm{Cf}_{\mathrm{adj,\,province}} = \mathrm{Cf}_{\mathrm{inv,province}} \times \left(\frac{\mathrm{Ns}_{\mathrm{province}}/\mathrm{POP}_{\mathrm{province}}}{2 \times \mathrm{Ns}_{\mathrm{nation}}/\mathrm{POP}_{\mathrm{nation}}} + \frac{\mathrm{Ve}_{\mathrm{province}}/\mathrm{POP}_{\mathrm{province}}}{2 \times \mathrm{Ve}_{\mathrm{nation}}/\mathrm{POP}_{\mathrm{nation}}} \right). \quad (10)$$

Here, Cf is the consumption of fireworks per capita, Ns is the number of retail shops selling fireworks, and Ve is the export volume of fireworks (from China Light Industry Yearbook data). In addition, the consumption (C) of sacrificial incense, joss paper, and fireworks at the municipal level was calculated by combining the POI data and the consumption at the provincial level, as shown in Eq. (11):

$$C_{\mathrm{adj,city}} = C_{\mathrm{inv,province}} \times \frac{N_{\mathrm{city}}/\mathrm{POP}_{\mathrm{city}}}{N_{\mathrm{province}}/\mathrm{POP}_{\mathrm{province}}}, \quad (11)$$

where N represents the number of temples or firework shops.

The original meat consumption information per capita was obtained from the statistical yearbook of each province. However, the methods and radii of the various provincial statistical yearbooks showed differences, and part of the municipal-level statistics was missing. To complement the missing data, the municipal per capita consumption expenditure was introduced. The logarithmic relationship between the per capita consumption expenditure and the provincial per capita meat consumption was adopted to complement municipal per capita meat consumption, as shown in Eq. (12):

$$y = a \times \ln x + b, \quad (12)$$

where x represents the provincial per capita consumption expenditure in 2000–2018, and y represents provincial per capita meat consumption in 2000–2018. The parameters a and b were the results derived by fitting Eq. (12) to the data for each province ($r = 0.60$, $p<0.01$), and a and b of the province where each city is located as well as the per capita consumption expenditure of the city were substituted into Eq. (12) to calculate the municipal per capita meat consumption.

2.4 Calculation of emissions

Some cities have established policies to forbid sacrificial incense, joss paper, and firework burning in the main urban area; however, such policies have been inoperative in nonurban regions. According to our survey, the policies forbidding sacrificial incense and joss paper burning have been relatively vague. We also assumed that if a city forbade fireworks, the burning of sacrificial incense and joss paper would also be banned. The total emissions (E) from sacrificial incense, joss paper, and fireworks were calculated as follows:

$$E = \sum (\mathrm{POP}_{\mathrm{urban},\,k} \times C_{\mathrm{urban},\,k} \times \mathrm{FB}_k + \mathrm{POP}_{\mathrm{nonurban},\,k} \times C_{\mathrm{nonurban},k}) \times \mathrm{EF}, \quad (13)$$

where k denotes the different cities; urban and nonurban represent urban regions and nonurban regions (rural regions), respectively; POP is the population; C is the per capita consumption; and EF is the emission factor. FB was either 0 or 1, depending on whether the burning of sacrificial incense, joss paper, and firework was forbidden in urban regions. Unfortunately, there were no detailed consumption data on sacrificial incense, joss paper, and firework fuel types. Thus, for the calculation of emissions from sacrificial incense, joss paper, and fireworks in this work, mean EFs were utilized.

Emissions from barbecue were calculated as follows:

$$E = \sum \left(\mathrm{POP}_{\mathrm{urban},\,k} \times \mathrm{MC}_{\mathrm{urban},\,k} + \mathrm{POP}_{\mathrm{nonurban},\,k} \times \mathrm{MC}_{\mathrm{nonurban},\,k}\right) \times \frac{T_{\mathrm{BBQ},k}}{T_{\mathrm{total},k}} \times \mathrm{OP} \times \mathrm{EF}, \quad (14)$$

where MC is the meat consumption mass per capita, T_{BBQ} is the number of restaurants specializing in barbecue, and T_{total} is the total number of restaurants. The number of restaurants was calculated using POI data. OP was the percentage of meals eaten out (according to National Institute for Nutrition and Health, Chinese Center for Disease Control and Prevention data). In this study, we assumed that barbecue was a kind of eating out.

Emissions from cooking were calculated as the sum of the emissions from residential cooking and emissions from the catering industry. They were calculated using Eqs. (15) and (16), respectively:

$$E_{\mathrm{RC}} = \sum \left(\mathrm{POP}_{\mathrm{urban},\,k} \times \mathrm{MC}_{\mathrm{urban},\,k} + \mathrm{POP}_{\mathrm{nonurban},\,k} \times \mathrm{MC}_{\mathrm{nonurban},\,k}\right) \times \left(1 - \frac{T_{\mathrm{BBQ},\,k}}{T_{\mathrm{total},k}}\right) \times (1 - \mathrm{OP}) \times \mathrm{EF} \times \mathrm{RE}_{\mathrm{RC},\,k}; \quad (15)$$

$$E_{\mathrm{CI}} = \sum \left(\mathrm{POP}_{\mathrm{urban},\,k} \times \mathrm{MC}_{\mathrm{urban},\,k} + \mathrm{POP}_{\mathrm{nonurban},\,k} \times \mathrm{MC}_{\mathrm{nonurban},\,k}\right) \times \left(1 - \frac{T_{\mathrm{BBQ},\,k}}{T_{\mathrm{total},k}}\right) \times \mathrm{OP} \times \mathrm{EF} \times \mathrm{RE}_{\mathrm{CI},\,k}. \quad (16)$$

Here, E_{RC} denotes emissions from residential cooking, E_{CI} denotes emissions from the catering industry, and RE is the removal efficiency. The removal efficiency for the catering industry ($\mathrm{RE}_{\mathrm{CI}}$) was obtained from the national standard (GB 18483-2001). The removal efficiency for residential cooking activity ($\mathrm{RE}_{\mathrm{RC}}$) was calculated using the rate of range hood adoption (based on China Statistical Yearbook data) and the removal efficiency of range hoods (national standard GB/T 17713-2011).

A Monte Carlo simulation was employed to analyze the uncertainties in the emission inventory (Wu et al., 2018). The simulation was executed 10 000 times. The uncertainties in the activity data were set as 0.2 or 0.5 (Table S1), and the uncertainties in the EFs were obtained from actual measurements. The resulting uncertainties are shown in Table S2.

2.5 Spatial–temporal distribution of emissions

As mentioned above, rural and urban activity resulting in emissions of the FMSs might differ greatly. During the process of spatial allocation, this difference must be emphasized. We used geographic information system (GIS) data for the classification of land use in order to divide regions into urban and nonurban areas (Gong et al., 2019, 2020). Based on this method, we obtained the data on the population distribution (data from http://worldpop.org, last access: 17 March 2021, https://doi.org/10.5258/SOTON/WP00674, WorldPop and Center for International Earth Science Information Network, 2018) in urban and rural regions and constructed the emission map of the FMSs (Sect. S4).

The temporal allocation methods for the FMSs were also specific. To calculate the annual emission trends, statistical data including annual firework sales (from Ministry of Emergency Management of the PRC data) and annual restaurant sales (from https://data.stats.gov.cn/, last access: 2 December 2020) were used. The monthly trends with respect to sacrificial incense, joss paper, and firework burning were calculated with data from household investigations. We believed that the activity of these sources are mainly concentrated on five traditional Chinese festivals: Chinese New Year's Eve (CNE), Chinese Spring Festival (CSF), Spring Lantern Festival (LF), Qingming Festival (QF), and Zhongyuan Festival (ZF) (Sect. S5). We calculated the percentage of incense, joss paper, and fireworks that burned during these festivals, and spread the excess to other days. The monthly trends with respect to barbecue and cooking emissions were calculated using the monthly restaurant sales in each province (from https://data.stats.gov.cn/, last access: 2 December 2020). It should be noted that the abovementioned methods were alternatives due to the lack of direct statistical data; thus, the methods can be improved in the future.

3 Results and discussion

3.1 Emission characterization and light absorption properties

The EFs obtained from the 38 tests are shown in Table 1. The mean $\mathrm{EF}_{\mathrm{OC}}$ values of sacrificial incense burning, barbecue, joss paper burning, firework burning, and cooking were 32.6 ± 12.6, 33.2 ± 13.5, 41.9 ± 27.8, 51.9 ± 45.5, and $159 \pm 34.0\ \mathrm{mg\,kg^{-1}}$, respectively. The $\mathrm{EF}_{\mathrm{EC}}$ and $\mathrm{EF}_{\mathrm{BC}}$ showed different tendencies: barbecue exhibited a higher $\mathrm{EF}_{\mathrm{EC}}$ and $\mathrm{EF}_{\mathrm{BC}}$ ($5.13 \pm 5.23\ \mathrm{mg\,kg^{-1}}$ and $69.6 \pm 79.5\ \mathrm{mg\,kg^{-1}}$, respectively) than those of sacrificial incense ($0.17 \pm 0.07\ \mathrm{mg\,kg^{-1}}$ and $1.80 \pm 0.92\ \mathrm{mg\,kg^{-1}}$, respectively), joss paper (2.25 ± 2.47 and $3.79 \pm 2.23\ \mathrm{mg\,kg^{-1}}$, respectively), cooking (0.005 ± 0.001 and $1.54 \pm 0.17\ \mathrm{mg\,kg^{-1}}$, respectively), and fireworks (2.57 ± 5.37 and $14.8 \pm 17.3\ \mathrm{mg\,kg^{-1}}$, respectively). Multiple factors, such as fuel properties (Chen

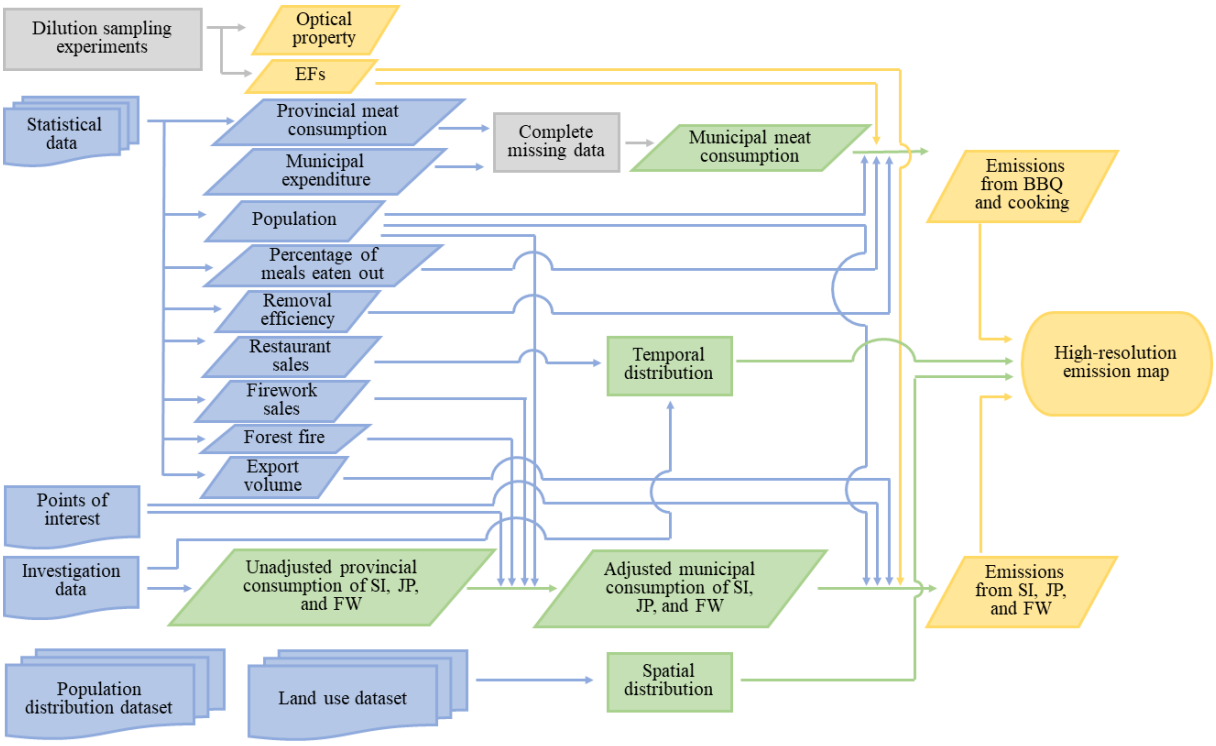

Figure 1. Methodological framework for establishing a high-resolution emission inventory for the five missing sources (FMSs).

et al., 2009; Shen et al., 2014; Cheng et al., 2019), combustion condition (Cheng et al., 2019), and stove properties (Shen et al., 2014; Chen et al., 2015), affected the emission of CAs from combustion sources. Similarly, CA emissions from the FMSs were dominated by diverse factors. The results from previous studies were also applicable in this study. For example, the emissions from environmental or aromatic incense were relatively low (Lee and Wang, 2004; Lui et al., 2016), and cooking fatty pork generated higher emissions (Saito et al., 2014). In addition, previous studies have shown higher EF_{OC} ($0.779\,g\,kg^{-1}$) and EF_{EC} ($0.339\,g\,kg^{-1}$) values for sacrificial offerings (S. Zhang et al., 2019). Huge differences in EFs are highly possible (Liu et al., 2015), and more detailed future research is needed to expand the datasets of EFs for the FMSs.

To quantify the light absorption properties of emissions from the FMSs, AAEs (370–880 nm) were calculated (Fig. 2). The average AAEs of the FMSs were in the range of 1.26–3.15. The mean AAE of sacrificial incense (2.69 ± 0.36) was slightly higher than that of joss paper (2.22 ± 0.65), fireworks (2.10 ± 0.50), barbecue (1.40 ± 0.14), and cooking (1.39 ± 0.08). The AAEs in the 370–880 nm wavelength for woody fuel burning (1.0–2.7) (Martinsson et al., 2015; A. Zhang et al., 2020; Z. Zhang et al., 2021), crop residue burning (1.5–3.25) (Tian et al., 2019; L. Zhang et al., 2020, 2021), coal combustion (1.1–2.5) (Tian et al., 2019; L. Zhang et al., 2021), and engines (1.1–2.4) (Corbin et al., 2018) were comparable to our results. AAE > 1 indicates that BrC is present in the aerosols (Saleh et al., 2013; Sun et al., 2017); thus, it is necessary to investigate BrC emission characteristics and the contribution of BrC to the total light absorption from various sources.

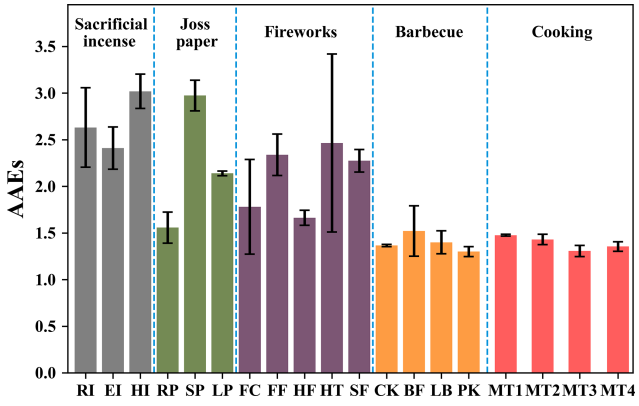

Figure 2. The absorption Ångström exponents (AAEs; 370–880 nm) of the FMSs.

We have calculated the f_{BrC} ($fBrC = 100\,\% \times babs(\lambda, BrC) / babs(\lambda)$) to estimate the light absorption ability of BrC in aerosols (Fig. S4). f_{BrC} showed a decreasing tendency toward the long wavelengths, which proved the understanding that the light absorption ability of BrC had stronger spectral dependence than that of BC (Sun et al., 2017). At the 370 nm wavelength, the f_{BrC} values of sacrificial in-

Table 1. Black carbon (BC), organic carbon (OC), and elemental carbon (EC) emission factors for the five missing sources (FMSs) (in mg kg^{-1}).

Sources	Materials	BC	OC	EC
Sacrificial incense	RI	3.09 ± 0.05	49.2 ± 6.39	0.23 ± 0.07
	EI	1.24 ± 0.17	27.3 ± 2.63	0.17 ± 0.02
	HI	1.07 ± 0.04	21.4 ± 2.06	0.10 ± 0.02
Joss paper	RP	6.27 ± 1.59	35.5 ± 5.59	0.97 ± 0.10
	SP	1.65 ± 0.41	14.6 ± 1.64	0.64 ± 0.50
	LP	3.45 ± 1.18	75.5 ± 19.2	5.12 ± 2.28
Fireworks	FC	3.56 ± 0.32	8.72 ± 0.08	0.14 ± 0.03
	FF	2.89 ± 0.88	5.86 ± 1.28	0.06 ± 0.03
	HF	23.0 ± 8.63	124 ± 29.2	9.79 ± 8.49
	HT	7.49 ± 0.20	65.7 ± 10.5	2.39 ± 1.76
	SF	37.3 ± 22.8	55.1 ± 0.66	0.48 ± 0.29
Barbecue	CK	1.66 ± 0.30	21.5 ± 1.11	0.15 ± 0.02
	BF	37.2 ± 24.4	28.6 ± 8.85	3.78 ± 2.28
	LB	48.5 ± 17.7	32.2 ± 6.35	4.21 ± 0.58
	PK	191 ± 59.5	50.5 ± 12.2	12.4 ± 4.93
Cooking	MT1	1.79 ± 0.04	127	0.003
	MT2	1.54 ± 0.01	124	0.004
	MT3	1.34 ± 0.05	181	0.007
	MT4	1.48 ± 0.07	203	0.007

The abbreviations used for fuels are as follows: RI – red incense; EI – environmental incense; HI – high incense; RP – red-printed paper; SP – small sacrificial paper; LP – large sacrificial paper; FC – firecrackers; FF – fountain fireworks; HF – handheld fireworks; HT – handheld fountain; SF – spin fireworks; CK – chicken; BF – beef; LB – lamb; PK – pork; MT1 – cooking of meat; MT2 – cooking of meat and pepper; MT3 – cooking of meat and garlic; and MT4 – cooking of meat, pepper, and garlic.

cense, joss paper, fireworks, barbecue, and cooking were 71.5 ± 5.32 %, 58.4 ± 24.0 %, 57.6 ± 9.36 %, 28.7 ± 6.19 %, and 29.2 ± 4.30 %, respectively. The f_{BrC} values of cooking sources (22.9 %–37.4 % with an average of 29.0 %), like barbecue and residential cooking, seemed to be much lower than that of other combustion sources (34.8 %–82.7 % with an average of 61.6 %). f_{BrC} values were 47 % for coal combustion at the 355 nm wavelength (Sun et al., 2017) and 68 %–85 % for biomass burning at 370 nm (Tian et al., 2019). As some emission sources were neglected, the particulate absorption and warming effect contributed by BrC may be underestimated in former modeling works (Laskin et al., 2015).

Furthermore, the AEFs of BrC and BC have been calculated, as shown in Fig. S5. As the wavelength increased, the AEFs showed a decreasing trend. When $\lambda = 370$ nm, AEF_{BrC} from fireworks was the highest (2.65 ± 3.23 m^2 kg^{-1}), followed by barbecue (0.45 ± 0.49 m^2 kg^{-1}), joss paper (0.19 ± 0.21 m^2 kg^{-1}), sacrificial incense (0.15 ± 0.10 m^2 kg^{-1}), and cooking (0.012 ± 0.004 m^2 kg^{-1}). At 370 nm, the AEF_{BrC} values of coal combustion and biomass burning have been reported to be 14.3–46.6 and 2.01–24 m^2 kg^{-1}, respectively (Martinsson et al., 2015; Tian et al., 2019), which are values 1–3 orders of magnitude higher than those of the FMSs.

3.2 Characterization of activity

The total consumption of the FMSs is shown in Fig. 3. In 2018, 16.5, 919, and 5139 kt of sacrificial incense, joss paper, and fireworks were burned in China, and 30 996, 2872, 1920, and 12 057 kt of pork, beef, lamb, and chicken were consumed. The total consumption of the abovementioned FMSs amounted to about 26.4 % of the residential coal consumption in China (Peng et al., 2019). The burning of sacrificial incense, joss paper, and fireworks was highest in Shandong (394 kt) and Sichuan (470 kt). Except for lamb, Guangdong Province has the highest consumption of three kinds of meats (6197 kt); the province with the highest consumption of lamb is Xinjiang (361 kt). The consumption of the FMSs can be a reflection of the local customs. For example, lamb consumption in Xinjiang is the highest in China. The reason for this may be that Xinjiang is the main lamb-producing area and one of the five main pastoral areas in China, and the region's ethnic structure makes mutton a dominant part of the daily diet (Xu et al., 2018).

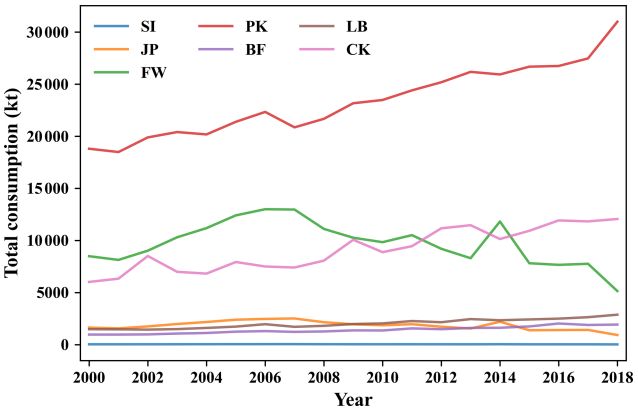

Figure 3. The total consumption of the FMSs in China during 2000–2018. The abbreviations used in the figure are as follows: SI – sacrificial incense, JP – joss paper, FW – fireworks, PK – pork, BF – beef, LB – lamb, and CK – chicken.

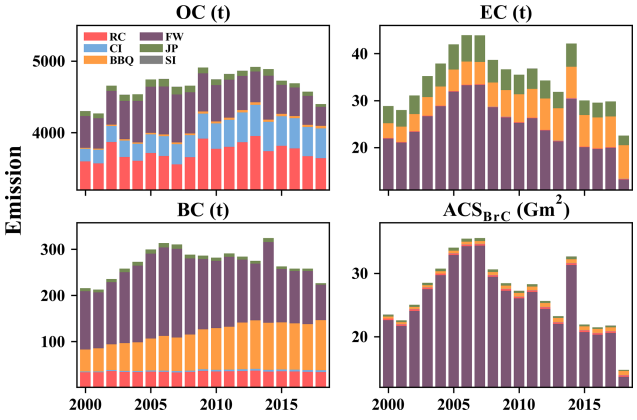

Figure 4. Total CA emissions from the FMSs in China from 2000 to 2018. The abbreviations used in the figure are as follows: SI – sacrificial incense, JP – joss paper, FW – fireworks, BBQ – barbecue, RC – residential cooking, and CI – catering industry.

The consumption of the FMSs in most cities was found to be low. The top 30 cities (about 8 % of the total number of cities) with the largest firework consumption contributed 41.8 % of the national consumption (Fig. S6). These cities have higher population densities, and control measures for fireworks were not in place at the time of study. Per capita firework consumption in 52 % of the cities was less than 5 kg yr^{-1}, and the mass of a common firecracker can exceeds 5 kg. As shown in Fig. S7, the distribution pattern of per capita consumption of sacrificial incense and joss paper was similar to that of fireworks. The differences in meat consumption between cities were relatively smaller. The top 30 cities with the largest pork consumption only contributed 30.8 % of the national consumption. The lowest per capita pork consumption was only 2.31 kg yr^{-1}, the highest was 45.6 kg yr^{-1} (Fig. S7), and 71.9 % of cities had a per capita pork consumption of between 10 and 30 kg yr^{-1}. From 2000 to 2018, the consumption of the four types of meat increased by 49.3 %, and the trends toward increased meat consumption were similar to a previous study (Batis et al., 2014). In contrast, the burning of sacrificial incense, joss paper, and fireworks first showed an increasing trend before changing to a decreasing trend.

3.3 CA emissions from the FMSs in China

3.3.1 Multiyear variation

In 2000–2018, the OC, EC, BC, and BrC absorption cross-section (ACS$_{BrC}$, in the 370 nm wavelength) emissions from the FMSs were 4268–4919 t, 22.6–43.9 t, 213–324 t, and 14.7–35.6 Gm^2, respectively (Fig. 4). Severe air pollution over the past decade has led China to enact a series of policies to limit emissions from various sources. Thus, the total CA emissions in China have presented approximately monotonically decreased tendencies. During 2010–2017, the total respective OC and BC emissions in China decreased from 3.2 and 1.7 Tg to 2.1 and 1.3 Tg, mostly contributed by residential sources (76.9 %–80.3 % of OC and 41.8 %–51.5 % of BC) (http://meicmodel.org, last access: 14 October 2021, Li et al., 2017; Zheng et al., 2018). The emissions of the FMSs have shown different variation tendencies compared with these above sources. A total of 82.7 %–92.3 % of OC emissions came from cooking (Fig. S8). Due to increased meat consumption (increase of 49 %) and the rate of range hood adoption (increase of 43.0 %), OC emissions from the FMSs increased by 14.4 % before 2013 and then decreased by 10.6 %. The EC, BC, and ACS$_{BrC}$ emissions showed similar tendencies. From 2000 to 2006, EC, BC, and ACS$_{BrC}$ emissions from the FMSs increased by 52.3 %, 45.4 %, and 51.2 %, respectively. They then decreased by 48.7 %, 27.8 %, and 58.4 %, respectively, in 2006–2018. Fireworks were one of the main contributors to CA emissions from the FMSs, contributing 58.6 %–76.0 %, 33.7 %–61.9 %, and 88.5 %–96.6 % of the respective EC, BC, and ACS$_{BrC}$ emissions. The consumption of fireworks showed an inverted U-shaped trend. Moreover, there was a surge in emissions due to the high consumption of fireworks in 2014, which is consistent with the temporal distribution of $PM_{2.5}$ (Sect. S6; Wei et al., 2020, 2021). This surge in sales might have been caused by destocking after the implementation of the Air Pollution Prevention and Control Action Plan (APPCP). Moreover, from 2000 to 2006, income increased by 76.5 % due to China's booming economy, and residents had more money to purchase fireworks. During this period, only 12 more cities forbade fireworks, which could be another reason for the increase in firework consumption amounts. From 2006 to 2018, although incomes continued to rise, the urbanization rate increased by 16.0 %, and an additional 201 cities forbade fireworks; this led to a decrease in firework consumption during this period.

3.3.2 Spatial variation

There are seven geographical regions in China (Fig. S9); of these areas, East China is the largest CA emission region, contributing 24.2 %–27.7 %, 23.9 %–29.6 %, 24.2 %–29.0 %, and 23.5 %–29.9 % of the OC, EC, BC, and ACS_{BrC} total emissions from the FMSs, respectively (Fig. 5). The dense population distribution (28.2 %–30.3 % of the population) is responsible for the high emissions in East China. The OC, EC, and BC emissions from the FMSs in Southwest China is second to that of East China. OC, EC, and BC emissions in Central China accounted for 21.5 %–27.2 %, 18.0 %–21.3 %, and 19.2 %–22.5 % of their national total emissions, respectively. Eating habits in Southwest China led to its high emission totals: Southwest China has a higher density of barbecue restaurants (11.9 % higher than the national average) and per capita meat consumption (33.4 % higher than the national average) as well as a large population (14.9 % of the national total). The ACS_{BrC} emissions from Central China are second to that of East China, accounting for 14.3 %–21.6 % of the national total. A total of 90.9 %–96.4 % of ACS_{BrC} emissions were from fireworks. Hunan Province, in Central China, is one of the main firework-producing regions. The density of firework stores in Hunan Province is 2.3 times the national average. Moreover, Central China is also one of the most densely populated regions in the country, accounting for 16.0 %–17.6 % of the national population. Due to heating requirements in winter, OC and BC emissions from other sources in North China contributed 14.8 %–17.2 % and 17.6 %–21.1 % of the national total, respectively (Li et al., 2017); however, the contributions of OC and BC emissions from the FMSs in North China were only 7.8 %–8.5 % and 9.5 %–10.5 %, respectively. This lower contribution was due to the lower per capita meat consumption (25.4 % lower than the national average) and the presence of fewer restaurants (5.5 % lower than the national average).

The emission distributions from different sources showed great differences, which stemmed from the regional cultural and economic diversity (Figs. S10, S11). High-emission regions with respect to sacrificial incense and joss paper burning overlapped with areas with large numbers of temples and cradles of Chinese Buddhism (Fig. S3, Sect. S7); people in these areas may be more devout about sacrifice. The distributions of cooking emissions (both residential cooking emissions and catering industry emissions) and barbecue emissions were highly similar to the population distribution, especially in urban regions. This is consistent with previous studies which reported that cooking-related organic aerosol (COA) concentrations at urban sites (6.46–6.97 in Beijing and 14.2 $\mu g\,m^{-3}$ in Shijiazhuang) were much higher than those at a rural site (2.96–3.74 $\mu g\,m^{-3}$ in Gucheng, near Beijing), and the COA concentration at the background site was zero (Sun et al., 2013, 2020; Q. Wang et al., 2015; Y. Wang et al., 2020; Huang et al., 2019). People in higher-income areas tend to have more uncommon dining habits, like barbecue, leading to higher emissions. Emissions from fireworks showed an obvious difference in urban and rural regions. Emissions from urban regions were near zero, whereas emissions from suburban and rural regions were much higher (more details can be found in Sect. 3.3.3 and Fig. 8).

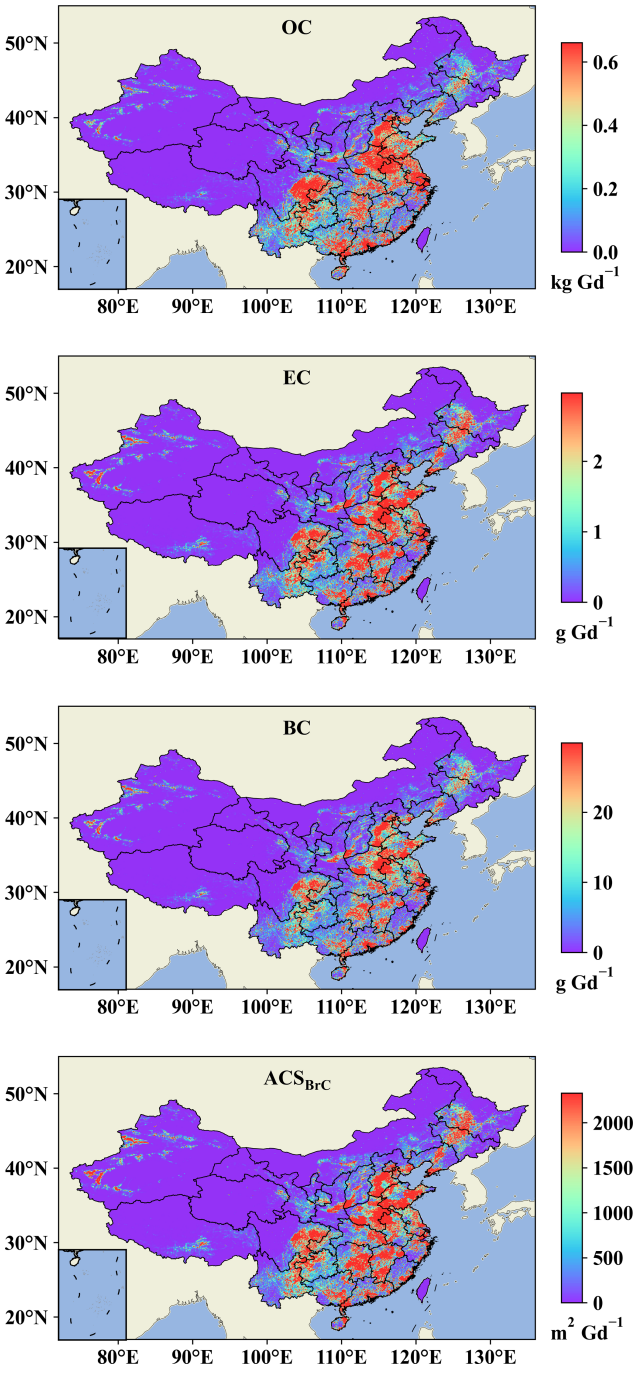

Figure 5. Spatial distribution of CA emissions from the FMSs in China in 2018. The color bar shows the emissions in each grid (where grid is denoted as Gd).

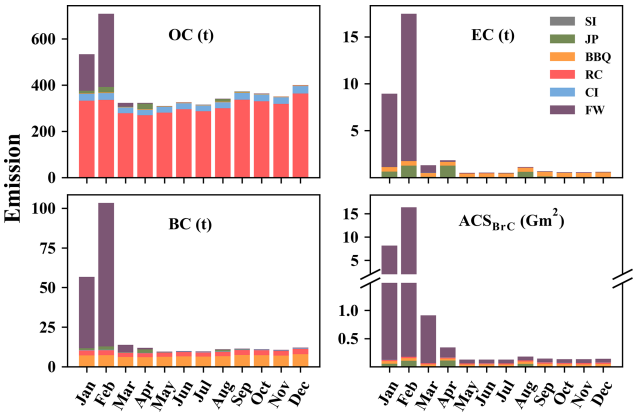

Figure 6. Averaged monthly CA emissions from the FMSs in China for the period from 2000 to 2018.

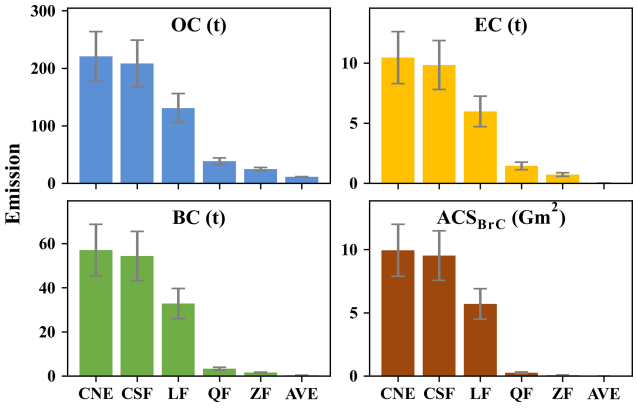

Figure 7. Average CA emissions during Chinese New Year's Eve (CNE), the Chinese Spring Festival (CSF), the Spring Lantern Festival (LF), the Qingming Festival (QF), and the Zhongyuan Festival (ZF) for the period from 2000 to 2018. AVE shows the average daily emissions for periods outside of the festivals mentioned above.

3.3.3 Intense short-term and regionally concentrated emissions

As shown in Figs. S12 and S13, CA emissions from residential sources in winter were much higher than those in summer due to the heating demand during the former season (Wang et al., 2012; Huang et al., 2015; Li et al., 2017), while emissions from the FMSs showed a similar seasonal trend due to fireworks. During the Chinese Spring Festival, fireworks result in massive pollutant emissions and severe air pollution (Kong et al., 2015; Yao et al., 2019; Ding et al., 2019; Lai and Brimblecombe, 2020). We have investigated the CA emissions from the FMSs in each month and during several related Chinese festivals (CNE, CSF, LF, QF, and ZF). As shown in Fig. 6, emissions were mostly concentrated in January and February (CNE and CSF are in the same month in 2000–2018); after the calculation of multiyear data, the results for January and February in Fig. 6 seemed to be lower than those in Fig. S13. A total of 75.8 % of fireworks were set off during CNE and CSF, and 20.4 % were set off during LF (Fig. 7). Thus, the ACS_{BrC} emissions during CNE were 1444 times the yearly average, and the OC, EC, and BC emissions were 10.9, 262, and 74.6 times the annual average, respectively. The high short-term emissions from fireworks led to a sharp increase in the concentration of air pollutants (Vecchi et al., 2008; Shi et al., 2011; Cao et al., 2018; Lai and Brimblecombe, 2020).

For a short-term period, emissions from the FMSs also showed an obvious spatial distribution. A total of 83.2 %–93.1 % of OC emissions came from barbecue and cooking. The higher population density and living quality led to higher OC emissions in urban regions. As shown in Fig. 8, the OC emission intensities (average emission per grid) in the urban regions of Chengdu, Xi'an, Beijing, and Tianjin were 62.6, 63.1, 27.0, and 14.6 times those in rural regions in 2018. This situation was common in China. Hence, China set up 13 prevention and control regions (3 key regions and 10 city clusters, referred to as 3-10R) in 2013 to improve air quality, and these areas were relatively developed regions (https://www.mee.gov.cn/gkml/hbb/bgg/201303/t20130305_248787.htm, last access: 16 April 2022). The OC emission intensities in the urban regions of 3-10R were 3.9–50.5 times higher than those in the surrounding rural regions. Thus, OC emissions from the FMSs were generally concentrated in urban regions. As firework use was concentrated during the CNE or CSF periods and in rural regions, the feature of OC emissions being concentrated in urban regions was attenuated during CNE. In contrast, ACS_{BrC} emissions tended to be concentrated in rural regions, especially during the CNE and CSF periods (Fig. 8). Fireworks were the main contributor (>88.5 %) to ACS_{BrC} emissions, and fireworks were concentrated during the CNE or CSF periods. The ACS_{BrC} emission intensities in the rural regions of Chengdu, Xi'an, Beijing, and Tianjin were 18.8, 20.0, 107, and 150 times higher than those in urban regions during CNE in 2018. However, many cities have introduced policies to control fireworks, and environmentally friendly sacrifice is encouraged. Nevertheless, these policies tend to be implemented effectively only in central urban regions. In suburbs and the surrounding rural regions, which are densely populated, policies may not be considered or executed efficiently. The contribution of rural ACS_{BrC} emissions in 3-10R was ∼79.0 % and even as high as 96.7 % during the 2018 CNE. However, the rural population in these regions only accounted for 14.1 %–41.9 % of their total population. In fact, 63.0 %–79.5 % of ACS_{BrC} emissions during CNE came from the rural regions in China. During the periods of CNE and CSF, pollutants emitted from rural residential activity were likely to be transmitted to urban areas, leading to serious air pollution in urban regions (Yao et al., 2019; Pang et al., 2021).

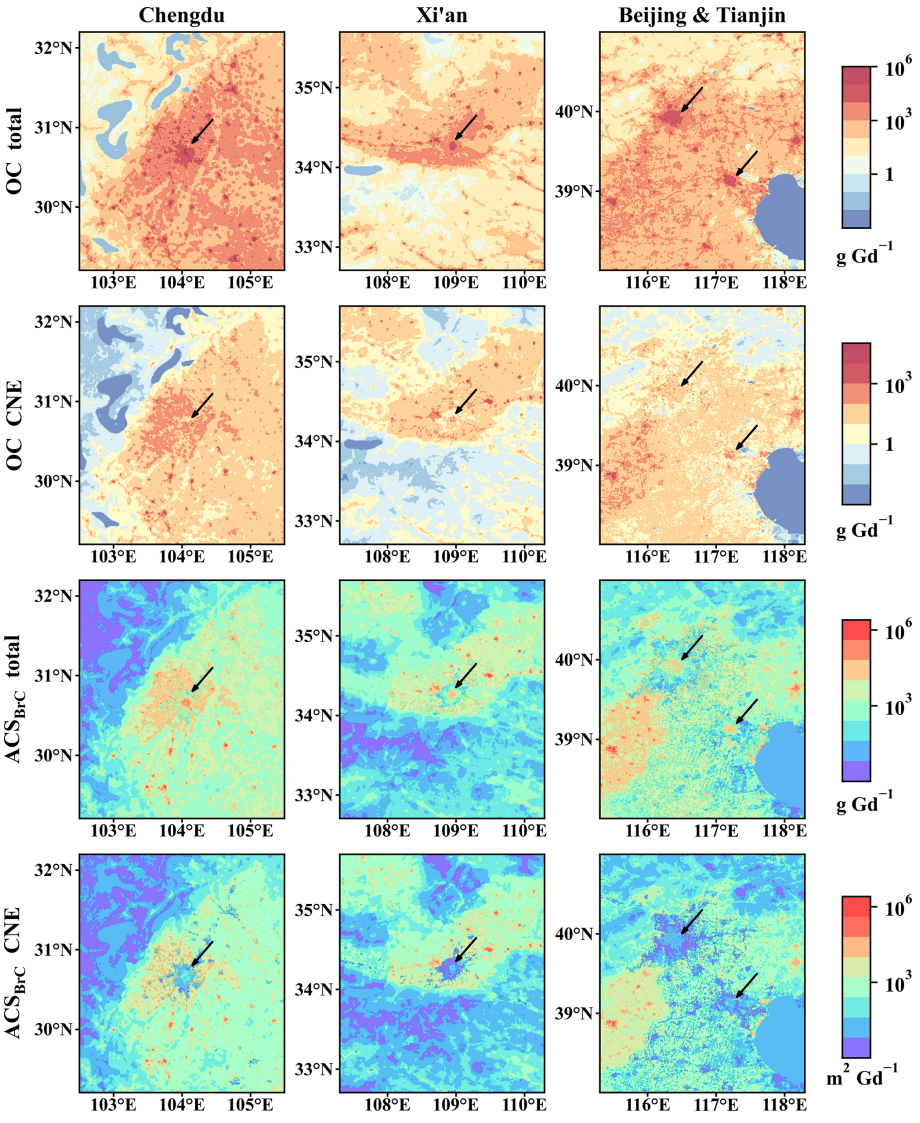

Figure 8. Differences in OC (top two rows) and ACS_{BrC} (bottom two rows) emission distributions in urban and rural regions in Chengdu (core city in the Sichuan Basin), Xi'an (core city on the Guanzhong Plain), and Beijing and Tianjin (core cities on the North China Plain). The first and second rows show the total OC emissions in 2018 and during CNE, respectively. The third and fourth rows show the ACS_{BrC} emissions in 2018 and during CNE, respectively. The arrows point to the city centers. The color bars show the emission in each grid (Gd) for OC and ACS_{BrC}.

3.3.4 Emissions impacted by economic development

Barbecue and cooking contributed a significant portion of OC emissions from the FMSs, which led to a distinctive feature of emissions from the FMSs: there was a certain correlation between OC emissions and local economic development. We gathered disposable income per capita data from 2000 to 2018 for each city, and the relationship between the disposable income and OC emissions per capita has been assessed. As shown in Fig. 9, like other emission sources, OC emissions from the FMSs and disposable income showed an inverted U-shaped relationship ($r^2 = 0.73$, $p<0.01$) (environmental Kuznets curves) (Wu et al., 2020; Zhong et al., 2020). This correlation existed for ACS_{BrC} emissions dominated by firework emissions, but the correlation was weaker ($r^2 = 0.59$, $p<0.01$) than that of OC emissions dominated by cooking sources. If we separated the emission–economy relationship in urban regions from that in rural regions, the results would be different. The relationships were linear in both urban and rural regions (Fig. 9); however, the correlation was significantly negative ($r = -0.97$, $p<0.01$) in urban regions compared with the positive relationship ($r = 0.94$, $p<0.01$) in rural regions. As discussed above, cooking sources dominated the OC emissions from the FMSs in China. From 2000 to 2018, meat consumption per capita increased by 83.4 %,

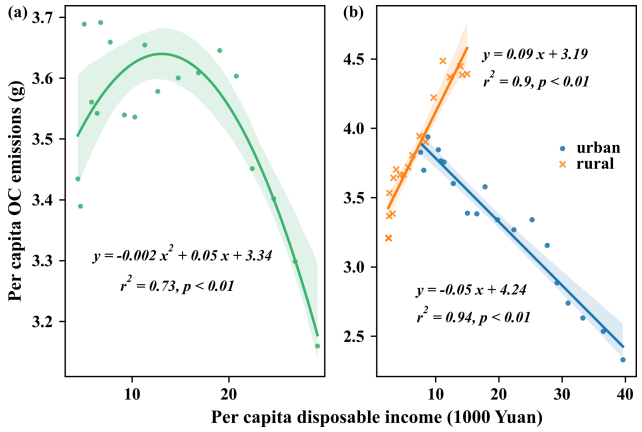

Figure 9. The relationship between the per capita disposable income and OC emissions from FMSs in China for the years from 2000 to 2018. Panel **(a)** shows the inverted U-shaped relationship between the income and the national average emissions. Panel **(b)** shows the correlation between income and emissions in urban and rural regions. The shaded areas represent the 95 % confidence intervals. Please note that "Yuan" in this figure refers to CNY.

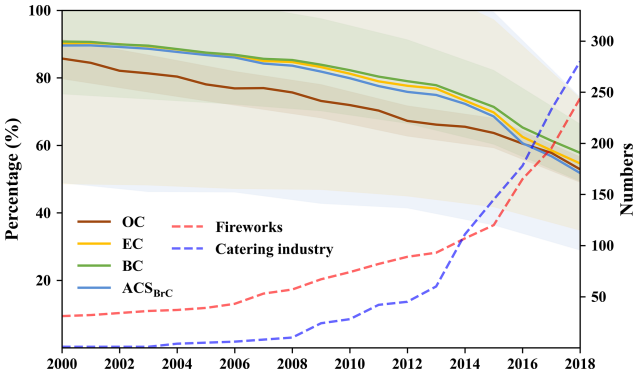

Figure 10. The impact of policies on the reduction of CA emissions. The solid lines (left *y* axis) represent the actual CA emissions compared with the emissions without the policy impact (100 % on the left *y* axis). The shaded part of the solid line represents uncertainties. The dotted lines (right *y* axis) represent the number of cities that issued policies to control the FMSs' emissions.

and the OC emissions per capita increased by 36.9 % in rural regions. In urban regions, meat consumption increased by 22.0 %, while OC emissions per capita decreased by 39.1 %. The reason for this phenomenon was the higher range hood adoption rate in urban regions, which was 5.2 times that of rural regions. Moreover, the range hood adoption rate in urban regions also increased by 132 % during this period. As a result, OC emissions that would have contributed to increasing emissions were instead eliminated by the large number of range hoods in these areas.

In contrast to the relatively developed 3-10R, there are some contiguous poor regions (CPRs) in China, located in the borderland or mountains (http://www.gov.cn/gzdt/2012-06/14/content_2161045.htm, last access: 29 March 2022). The other regions (ORs) in China, excluding 3-10R and the CPRs, are at a moderate level of development. The OC emissions per capita in 3-10R, the ORs, and the CPRs, were 3.04–3.77, 3.49–4.00, and 3.54–4.11 g in 2000–2018, respectively. OC emissions per capita in 3-10R, the ORs, and the CPRs have all crossed the inflection point of the emission–economy correlation. Thus, the relatively developed 3-10R has lower per capita emissions. This also verifies the economic impact of OC emissions. However, 3-10R is home to 76.2 %–77.4 % of the population; thus, the emission intensities in 3-10R are still 3.1–3.4 times that of the national average.

3.3.5 The implication of modifying related air pollution control policies

To combat air pollution, China introduced its toughest air pollution control plan (APPCP) ever in 2013 (Q. Zhang et al., 2019). The implementation of the APPCP has led to significant improvements in China's air quality. Measures to control the FMSs have also begun to be widely promoted (Fig. S14). A total of 76.3 % and 66.5 % of cities had introduced policies to restrict emissions from the catering industry and fireworks, respectively, before 2018. The pollutant removal efficiencies of small, medium, and large catering businesses are higher than 60 %, 75 %, and 85 %, respectively (national standard GB 18483-2001). Local governments have the right to designate areas in which fireworks are forbidden: these are usually urban areas as well as hospitals, factories, power plants, schools, and transportation hubs (http://www.gov.cn/zwgk/2006-01/25/content_170906.htm, last access: 3 May 2022). In addition, in the APPCP, the government proposed that residents install range hoods to control the emissions from cooking, and the national range hood adoption rate subsequently increased by 43.6 % from 2000 to 2018. The control policies and recommendations mentioned above have been implemented at various times in different cities, and they all have positive significance with respect to emission reduction. As a result, OC, EC, BC, and ACS$_{BrC}$ emissions from the FMSs have declined by 14.3 %–47.1 %, 9.8 %–45.4 %, 9.2 %–42.2 %, and 10.4 %–48.2 %, respectively, between 2000 and 2018 (Fig. 10).

If we assume that there is also a quadratic fitting relationship between the rural per capita OC emissions and income, the rural per capita OC emissions would start to decline when the rural per capita income reaches CNY 16 800. The control of CA emissions from the FMSs, such as cooking, should start from the perspective of increasing the income of rural residents. With sufficient income, residents will tend toward a more environmentally friendly and green lifestyle. In this case, a green lifestyle is embodied by the installation of a range hood. In 2017, the impervious surfaces of urban regions only accounted for 1.52 % of the national area (Gong

et al., 2019), and rural regions were vast by contrast. Thus, the cost of controlling firework, sacrificial incense, and joss paper burning activity in rural regions will be much higher than in urban regions. For these sources, policies and standards should be set to limit their emissions. In addition, it is questionable whether the environmentally friendly fireworks currently on the market have a lower impact on the environment (Fan et al., 2021). Thus, manufacturers should be guided toward the development of environmentally friendly fireworks, joss paper, and sacrificial incense in order to reduce emissions.

3.4 Comparison with other studies

Most of the relevant existing studies on emissions have focused on the EFs of PM (Jetter et al., 2002; Lee and Wang, 2004; G. Wang et al., 2015; Kuo et al., 2016; Jilla and Kura, 2017; Amouei Torkmahalleh et al., 2018; L. Wang et al., 2018; Zhao et al., 2018; Lin et al., 2019), PAHs (Yang et al., 2005, 2013; Zhao et al., 2019), and volatile organic compounds (VOCs) (Cheng et al., 2016; L. Wang et al., 2018). Several metallic elements (Croteau et al., 2010; Shen et al., 2017) and organic matter components (Xiang et al., 2017; Que et al., 2019) have also been tested. However, few studies have tested the OC and EC EFs of the FMSs (See and Balasubramanian, 2011; S. Zhang et al., 2019; Lin et al., 2021). Fireworks are the least-studied emission source, although they can emit large amounts of particles. EFs of PM_{10} from fireworks as high as 54–429 $g\,kg^{-1}$ have been reported (Camilleri and Vella, 2016; Keller and Schragen, 2021), which are much higher values than the CA EFs in this study. EFs in the existing literature are shown in Table S4.

Several studies have calculated the emission amount of the catering industry (Table S5). For example, H. Wang et al. (2018) calculated the VOC emissions (66 245 t) from restaurants in China based on samples taken from nine types of restaurants. Jin et al. (2021) calculated the OC emissions from the catering industry in China by undertaking investigations in two cities in the Shandong and Shanxi provinces. The results showed that OC emissions from the catering industry were 26.8 Gg, which was 66.0 times the values obtained in this work. The EFs used in Jin et al. (2021) were the generation rates of pollutants, which were 0.48 $mg\,m^{-3}$ for OC in oil fumes. Different EFs and calculation methods may be the main reason for the abovementioned discrepancies. Emissions from cooking have been reported as the main driver of OC in urban regions, and they have been found to contribute large portions of the organic aerosols measured in Shanghai (20 %–35 %) and Beijing (10 %–19 %) (Liu et al., 2021; Zhu et al., 2021b). The effects of cooking emissions on the urban atmosphere should not be neglected when other sources like residential or industry sources are being efficiently controlled (Z. Zhang et al., 2021; Zhu et al., 2021a).

Previous research has calculated the total OC and BC emissions in China, such as the widely used the Multi-resolution Emission Inventory for China (MEIC) (OC: 2080–3190 Gg; BC: 1253–1728 Gg) and the Peking University (PKU) (OC: 2345–3587 Gg; BC: 1455–1624 Gg) emission inventories (R. Wang et al., 2014; Huang et al., 2015; Li et al., 2017). Residential sources or residential and commercial sources contributed most of the OC (80.3 % in MEIC and 71.4 % in PKU) and BC (51.5 % in MEIC and 51.0 % in PKU) emissions (Peng et al., 2019). The OC and BC emissions from the FMSs accounted for only 1.5 ‰–2.2 ‰ and 0.16 ‰–0.20 ‰ of their national total emissions. Thus, the OC and BC emissions from the FMSs were generally meager. During key periods, like the CNE, the contributions of the FMSs to the total OC and BC emissions can rise to 2.3 %–3.5 % and 1.1 %–1.6 %, respectively. In key areas, the contribution rates would be relatively higher. For instance, during the 2014 CNE, the FMSs contributed 6.3 % of the OC emissions in the Sichuan Basin and 2.9 % of the BC emissions in the Jiangxi–Hunan area. However, it should be noted that the fireworks were always set off from about 20:00 to 00:00 LT (local time) during the CNE; thus, intense emission amounts could be expected during this period. Therefore, the contribution of fireworks to CAs in the atmosphere during the CNE and CSF is still a topic of debate.

Widespread controversy has also stemmed from the fact that the government chooses not to control emissions from industry and vehicles during CNE but emphasizes controls on the emissions from fireworks. The public can not accept or believe that the emissions from fireworks can lead to serious air pollution, which could be a key reason why they can not be completely eradicated in cities. From this study, it can be seen that CA emissions are limited compared with those from residential sources. An interesting question that atmospheric scientists needed answer in the future is "If fireworks were not controlled, how many air pollutants from other major urban sources should be alternatively controlled in cities?".

4 Data availability

The dataset generated in this work is available at https://doi.org/10.6084/m9.figshare.19999991.v2 (Cheng et al., 2022): POI (locations of barbecue restaurants, temples, common restaurants, and firework shops) data were obtained from Amap (https://lbs.amap.com/, Amap, 2021); data from the China Forestry Statistical Yearbook (forest fires and the rate of range hood adoption), the China Light Industry Yearbook (firework export volume), and the statistical yearbook of each province (urban and rural population, meat consumption, consumption expenditure, and disposable income) were obtained from https://data.cnki.net (CNKI, 2020); data regarding the percentage of meals eaten out were obtained from https://www.chinanutri.cn/ (National Institute for Nutrition and Health, Chinese Center for Disease Control and Prevention, 2021); population data were obtained from https://doi.org/10.5258/SOTON/WP00674 (WorldPop

and Center for International Earth Science Information Network, 2018); land use data were sourced from http://data.ess.tsinghua.edu.cn/ (Gong et al., 2019, 2020); data on annual fireworks sales were obtained from https://www.mem.gov.cn/gk/tjsj/ (Ministry of Emergency Management of the PRC, 2020); and annual and monthly restaurant sale data were sourced from https://data.stats.gov.cn/ (National Bureau of Statistics, 2020).

5 Summary and conclusions

The absence of anthropogenic sources in the existing inventories prevents people from drawing accurate conclusions about the control of short-term pollution. To calculate the emissions from these sources, which are difficult to estimate, we construct an emission inventory establishment framework, including a series of equations and methods. We use multiple proxy data, such as questionnaire data, various statistical data, and points of interest data, to build a dataset of the activity of the five missing sources (FMSs, including cooking, fireworks, sacrificial incense and joss paper burning, and barbecue). The carbonaceous aerosol (CA) emission factors were tested in our lab using a custom-made sampling platform. The OC, EC, and BC EFs were 5.86–203, 0.003–12.4m and 1.07–191 mg kg^{-1}, respectively. BrC absorption EFs were in the range of 0.01–6.05 m^2 kg^{-1} (370 nm). From 2000 to 2018, the activity of the FMSs emitted 4268–4919, 22.6–43.9, 213–324 t, and 14.7–35.6 Gm^2 of OC, EC, BC, and BrC absorption cross-section (ACS_{BrC}, in 370 nm wavelength), respectively. Emissions from the FMSs were concentrated around special festivals; for example, CA emissions on Chinese New Year's Eve were more than 10.8 times their annual average. The distribution of pollutants also showed great differences between urban and rural regions due to variations in demographics, economic situations, and policy implications. There was a negative correlation ($r = -0.97$, $p<0.01$) between individual emissions and disposable income in rural areas and a positive correlation ($r = 0.94$, $p<0.01$) in urban areas. The policy implications led to a CA emission reduction of over 42.2 % with respect to the FMSs. This study complements the lack of emission inventory research on such missing sources and provides the prerequisite for modeling studies. Meanwhile, we suggest that increasing the population's income would be a feasible solution with respect to reducing the emissions of FMSs that are difficult to control. Fireworks can be controlled from the manufacturer's side by guiding them toward the development of more environmentally friendly products. We also question whether it may be possible to control other emission sources in order to provide the environmental capacity for firework emissions.

Supplement. The supplement related to this article is available online at: https://doi.org/10.5194/essd-14-4757-2022-supplement.

Author contributions. YC was responsible for carrying out the experiments, processing the data, and writing the manuscript. SK conceptualized the study, developed the methodology, supervised the study, and reviewed and edited the manuscript. LY and HZ participated in the experiments, and LY, HZ, and JW undertook the formal analysis. QY, SZ, and ZN participated in experiments. YH was responsible for validation of the results. YY, ZS, GS, DL, SW, and SQ supervised the study.

Competing interests. The contact author has declared that none of the authors has any competing interests.

Disclaimer. Publisher's note: Copernicus Publications remains neutral with regard to jurisdictional claims in published maps and institutional affiliations.

Financial support. This study was supported by the National Natural Science Foundation of China (grant nos. 42077202 and 41830965) and the Key Program of the Ministry of Science and Technology of the People's Republic of China (grant nos. 2016YFA0602002 and 2017YFC0212602).

Review statement. This paper was edited by Bo Zheng and reviewed by two anonymous referees.

References

Amap: Amap Web service API, https://lbs.amap.com/, last access 6 April 2021.

Amouei Torkmahalleh, M., Ospanova, S., Baibatyrova, A., Nurbay, S., Zhanakhmet, G., and Shah, D.: Contributions of burner, pan, meat and salt to PM emission during grilling, Environ. Res., 164, 11–17, https://doi.org/10.1016/j.envres.2018.01.044, 2018.

Batis, C., Sotres-Alvarez, D., Gordon-Larsen, P., Mendez, M. A., Adair, L., and Popkin, B.: Longitudinal analysis of dietary patterns in Chinese adults from 1991 to 2009, Br. J. Nutr., 111, 1441–1451, https://doi.org/10.1017/S0007114513003917, 2014.

Bond, T. C., Doherty, S. J., Fahey, D. W., Forster, P. M., Berntsen, T., DeAngelo, B. J., Flanner, M. G., Ghan, S., Kärcher, B., Koch, D., Kinne, S., Kondo, Y., Quinn, P. K., Sarofim, M. C., Schultz, M. G., Schulz, M., Venkataraman, C., Zhang, H., Zhang, S., Bellouin, N., Guttikunda, S. K., Hopke, P. K., Jacobson, M. Z., Kaiser, J. W., Klimont, Z., Lohmann, U., Schwarz, J. P., Shindell, D., Storelvmo, T., Warren, S. G., and Zender, C. S.: Bounding the role of black carbon in the climate system: A scientific assessment, J. Geophys. Res.-Atmos., 118, 5380–5552, https://doi.org/10.1002/jgrd.50171, 2013.

Camilleri, R. and Vella, A. J.: Emission factors for aerial pyrotechnics and use in assessing environmental impact of firework displays: Case study from Malta, Prop. Explos. Pyrotech., 41, 273–280, https://doi.org/10.1002/prep.201500205, 2016.

Cao, X., Zhang, X., Tong, D. Q., Chen, W., Zhang, S., Zhao, H., and Xiu, A.: Review on physicochemical properties of pollutants released from fireworks: Environmental and health effects and pre-

vention, Environ. Rev., 26, 133–155, https://doi.org/10.1139/er-2017-0063, 2018.

Chen, Y., Zhi, G., Feng, Y., Liu, D., Zhang, G., Li, J., Sheng, G., and Fu, J.: Measurements of black and organic carbon emission factors for household coal combustion in China: Implication for emission reduction, Environ. Sci. Technol., 43, 9495–9500, https://doi.org/10.1021/es9021766, 2009.

Chen, Y., Tian, C., Feng, Y., Zhi, G., Li, J., and Zhang, G.: Measurements of emission factors of $PM_{2.5}$, OC, EC, and BC for household stoves of coal combustion in China, Atmos. Environ., 109, 190–196, https://doi.org/10.1016/j.atmosenv.2015.03.023, 2015.

Cheng, S., Wang, G., Lang, J., Wen, W., Wang, X., and Yao, S.: Characterization of volatile organic compounds from different cooking emissions, Atmos. Environ., 145, 299–307, https://doi.org/10.1016/j.atmosenv.2016.09.037, 2016.

Cheng, Y., Kong, S., Yan, Q., Liu, H., Wang, W., Chen, K., Yin, Y., Zheng, H., Wu, J., Yao, L., Zeng, X., Zheng, S., Wu, F., Niu, Z., Zhang, Y., Yan, Y., Zheng, M., and Qi, S.: Size-segregated emission factors and health risks of PAHs from residential coal flaming/smoldering combustion, Environ. Sci. Pollut. Res., 26, 31793–31803, https://doi.org/10.1007/s11356-019-06340-2, 2019.

Cheng, Y., Kong, S., Yao, L., Zheng, H., Wu, J., Yan, Q., Zheng, S., Hu, Y., Niu, Z., Yan, Y., Shen, Z., Shen, G., Liu, D., Wang, S., and Qi, S.: Multi-year emission of carbonaceous aerosols from cooking, fireworks burning, sacrificial incenses, joss paper burning, and barbecue and the key driving forces in China, Figshare [data set], https://doi.org/10.6084/m9.figshare.19999991.v2, 2022.

Chiang, K.-C. and Liao, C.-M.: Heavy incense burning in temples promotes exposure risk from airborne PMs and carcinogenic PAHs, Sci. Total Environ., 372, 64–75, https://doi.org/10.1016/j.scitotenv.2006.08.012, 2006.

CNKI: China's economic and social big data research platform, https://data.cnki.net, last access: 21 October 2020.

Corbin, J. C., Pieber, S. M., Czech, H., Zanatta, M., Jakobi, G., Massabò, D., Orasche, J., El Haddad, I., Mensah, A. A., Stengel, B., Drinovec, L., Mocnik, G., Zimmermann, R., Prévôt, A. S. H., and Gysel, M.: Brown and black carbon emitted by a marine engine operated on heavy fuel oil and distillate fuels: Optical properties, size distributions, and emission factors, J. Geophys. Res.-Atmos., 123, 6175–6195, https://doi.org/10.1029/2017JD027818, 2018.

Croteau, G., Dills, R., Beaudreau, M., and Davis, M.: Emission factors and exposures from ground-level pyrotechnics, Atmos. Environ., 44, 3295–3303, https://doi.org/10.1016/j.atmosenv.2010.05.048, 2010.

Ding, J., Guo, J., Wang, L., Chen, Y., Hu, B., Li, Y., Huang, R., Cao, J., Zhao, Y., Geiser, M., Miao, Q., Liu, Y., and Chen, C.: Cellular responses to exposure to outdoor air from the Chinese Spring Festival at the air–liquid interface, Environ. Sci. Technol., 53, 9128–9138, https://doi.org/10.1021/acs.est.9b00399, 2019.

Ding, Q., Liu, J., Lu, Y., Wang, Y., Lu, F., and Shi, J.: Research and development of an on-line carbonaceous aerosol analyzer (In Chinese), Chin. J. Sci. Instrum., 35, 1246–1253, https://doi.org/10.19650/j.cnki.cjsi.2014.06.007, 2014.

Drinovec, L., Močnik, G., Zotter, P., Prévôt, A. S. H., Ruckstuhl, C., Coz, E., Rupakheti, M., Sciare, J., Müller, T., Wiedensohler, A., and Hansen, A. D. A.: The "dual-spot" Aethalometer: an improved measurement of aerosol black carbon with real-time loading compensation, Atmos. Meas. Tech., 8, 1965–1979, https://doi.org/10.5194/amt-8-1965-2015, 2015.

Fan, S., Li, Y., and Liu, C.: Are environmentally friendly fireworks really "green" for air quality? A study from the 2019 National Day fireworks display in Shenzhen, Environ. Sci. Technol., 55, 3520–3529, https://doi.org/10.1021/acs.est.0c03521, 2021.

Feng, Y., Ramanathan, V., and Kotamarthi, V. R.: Brown carbon: a significant atmospheric absorber of solar radiation?, Atmos. Chem. Phys., 13, 8607–8621, https://doi.org/10.5194/acp-13-8607-2013, 2013.

Gong, P., Li, X., and Zhang, W.: 40-Year (1978–2017) human settlement changes in China reflected by impervious surfaces from satellite remote sensing, Sci. Bull., 64, 756–763, https://doi.org/10.1016/j.scib.2019.04.024, 2019 (data available at: http://data.ess.tsinghua.edu.cn/, last access: 15 March 2021).

Gong, P., Chen, B., Li, X., Liu, H., Wang, J., Bai, Y., Chen, J., Chen, X., Fang, L., Feng, S., Feng, Y., Gong, Y., Gu, H., Huang, H., Huang, X., Jiao, H., Kang, Y., Lei, G., Li, A., Li, X., Li, X., Li, Y., Li, Z., Li, Z., Liu, C., Liu, C., Liu, M., Liu, S., Mao, W., Miao, C., Ni, H., Pan, Q., Qi, S., Ren, Z., Shan, Z., Shen, S., Shi, M., Song, Y., Su, M., Ping Suen, H., Sun, B., Sun, F., Sun, J., Sun, L., Sun, W., Tian, T., Tong, X., Tseng, Y., Tu, Y., Wang, H., Wang, L., Wang, X., Wang, Z., Wu, T., Xie, Y., Yang, J., Yang, J., Yuan, M., Yue, W., Zeng, H., Zhang, K., Zhang, N., Zhang, T., Zhang, Y., Zhao, F., Zheng, Y., Zhou, Q., Clinton, N., Zhu, Z., and Xu, B.: Mapping essential urban land use categories in China (EULUC-China): Preliminary results for 2018, Sci. Bull., 65, 182–187, https://doi.org/10.1016/j.scib.2019.12.007, 2020 (data available at: http://data.ess.tsinghua.edu.cn/, last access: 15 March 2021).

Ho, C.-C., Chan, C.-C., Chio, C.-P., Lai, Y.-C., Chang-Chien, G.-P., Chow, J. C., Watson, J. G., Chen, L.-W. A., Chen, P.-C., and Wu, C.-F.: Source apportionment of mass concentration and inhalation risk with long-term ambient PCDD/Fs measurements in an urban area, J. Hazard. Mater., 317, 180–187, https://doi.org/10.1016/j.jhazmat.2016.05.059, 2016.

Hu, R., Wang, S., Zheng, H., Zhao, B., Liang, C., Chang, X., Jiang, Y., Yin, R., Jiang, J., and Hao, J.: Variations and sources of organic aerosol in winter Beijing under markedly reduced anthropogenic activities during COVID-2019, Environ. Sci. Technol., 56, 6956–6967, https://doi.org/10.1021/acs.est.1c05125, 2021.

Huang, D. D., Zhu, S., An, J., Wang, Q., Qiao, L., Zhou, M., He, X., Ma, Y., Sun, Y., Huang, C., Yu, J. Z., and Zhang, Q.: Comparative assessment of cooking emission contributions to urban organic aerosol using online molecular tracers and Aerosol Mass Spectrometry measurements, Environ. Sci. Technol., 55, 14526–14535, https://doi.org/10.1021/acs.est.1c03280, 2021.

Huang, R.-J., Wang, Y., Cao, J., Lin, C., Duan, J., Chen, Q., Li, Y., Gu, Y., Yan, J., Xu, W., Fröhlich, R., Canonaco, F., Bozzetti, C., Ovadnevaite, J., Ceburnis, D., Canagaratna, M. R., Jayne, J., Worsnop, D. R., El-Haddad, I., Prévôt, A. S. H., and O'Dowd, C. D.: Primary emissions versus secondary formation of fine particulate matter in the most polluted city (Shijiazhuang) in North China, Atmos. Chem. Phys., 19, 2283–2298, https://doi.org/10.5194/acp-19-2283-2019, 2019.

Huang, Y., Shen, H., Chen, Y., Zhong, Q., Chen, H., Wang, R., Shen, G., Liu, J., Li, B., and Tao, S.: Global organic carbon emissions from primary sources from 1960 to 2009, Atmos. Environ., 122, 505–512, https://doi.org/10.1016/j.atmosenv.2015.10.017, 2015.

Janssens-Maenhout, G., Crippa, M., Guizzardi, D., Muntean, M., Schaaf, E., Dentener, F., Bergamaschi, P., Pagliari, V., Olivier, J. G. J., Peters, J. A. H. W., van Aardenne, J. A., Monni, S., Doering, U., Petrescu, A. M. R., Solazzo, E., and Oreggioni, G. D.: EDGAR v4.3.2 Global Atlas of the three major greenhouse gas emissions for the period 1970–2012, Earth Syst. Sci. Data, 11, 959–1002, https://doi.org/10.5194/essd-11-959-2019, 2019.

Jetter, J. J., Guo, Z., McBrian, J. A., and Flynn, M. R.: Characterization of emissions from burning incense, Sci. Total Environ., 295, 51–67, https://doi.org/10.1016/S0048-9697(02)00043-8, 2002.

Jilla, A. and Kura, B.: Particulate matter and carbon monoxide emission factors from incense burning, Environ. Pollut. Clim. Chang., 1, 1000140, https://doi.org/10.4172/2573-458X.1000140, 2017.

Jin, W., Zhi, G., Zhang, Y., Wang, L., Guo, S., Zhang, Y., Xue, Z., Zhang, X., Du, J., Zhang, H., Ren, Y., Xu, P., Ma, J., Zhao, W., Wang, L., and Fu, R.: Toward a national emission inventory for the catering industry in China, Sci. Total Environ., 754, 142184, https://doi.org/10.1016/j.scitotenv.2020.142184, 2021.

Keller, F. and Schragen, C.: Determination of particulate matter emission factors of common pyrotechnic articles, Prop. Explos. Pyrotech., 46, 825–842, https://doi.org/10.1002/prep.202000292, 2021.

Kong, S. F., Li, L., Li, X. X., Yin, Y., Chen, K., Liu, D. T., Yuan, L., Zhang, Y. J., Shan, Y. P., and Ji, Y. Q.: The impacts of firework burning at the Chinese Spring Festival on air quality: insights of tracers, source evolution and aging processes, Atmos. Chem. Phys., 15, 2167–2184, https://doi.org/10.5194/acp-15-2167-2015, 2015.

Kuo, S.-C., Tsai, Y. I., and Sopajaree, K.: Emission characteristics of carboxylates in $PM_{2.5}$ from incense burning with the effect of light on acetate, Atmos. Environ., 138, 125–134, https://doi.org/10.1016/j.atmosenv.2016.05.004, 2016.

Lai, Y. and Brimblecombe, P.: Changes in air pollution and attitude to fireworks in Beijing, Atmos. Environ., 231, 117549, https://doi.org/10.1016/j.atmosenv.2020.117549, 2020.

Lao, J.-Y., Xie, S.-Y., Wu, C.-C., Bao, L.-J., Tao, S., and Zeng, E. Y.: Importance of dermal absorption of polycyclic aromatic hydrocarbons derived from barbecue fumes, Environ. Sci. Technol., 52, 8330–8338, https://doi.org/10.1021/acs.est.8b01689, 2018.

Laskin, A., Laskin, J., and Nizkorodov, S. A.: Chemistry of atmospheric brown carbon, Chem. Rev., 115, 4335–4382, https://doi.org/10.1021/cr5006167, 2015.

Lee, S.-C. and Wang, B.: Characteristics of emissions of air pollutants from burning of incense in a large environmental chamber, Atmos. Environ., 38, 941–951, https://doi.org/10.1016/j.atmosenv.2003.11.002, 2004.

Li, M., Liu, H., Geng, G., Hong, C., Liu, F., Song, Y., Tong, D., Zheng, B., Cui, H., Man, H., Zhang, Q., and He, K.: Anthropogenic emission inventories in China: A review, Natl. Sci. Rev., 4, 834–866, https://doi.org/10.1093/nsr/nwx150, 2017.

Liakakou, E., Kaskaoutis, D. G., Grivas, G., Stavroulas, I., Tsagkaraki, D., Paraskevopoulou, D., Bougiatioti, A., Dumka, U. C., Gerasopoulos, E., and Mihalopoulos, N.: Long-term brown carbon spectral characteristics in a Mediterranean city (Athens), Sci. Total Environ., 708, 135019, https://doi.org/10.1016/j.scitotenv.2019.135019, 2020.

Lin, M.-D., Rau, J.-Y., Tseng, H.-H., Wey, M.-Y., Chu, C.-W., Lin, Y.-H., Wei, M.-C., and Lee, C.-H.: Characterizing PAH emission concentrations in ambient air during a large-scale joss paper open-burning event, J. Hazard. Mater., 156, 223–229, https://doi.org/10.1016/j.jhazmat.2007.12.015, 2008.

Lin, P., He, W., Nie, L., Schauer, J. J., Wang, Y., Yang, S., and Zhang, Y.: Comparison of $PM_{2.5}$ emission rates and source profiles for traditional Chinese cooking styles, Environ. Sci. Pollut. Res., 26, 21239–21252, https://doi.org/10.1007/s11356-019-05193-z, 2019.

Lin, P., Gao, J., He, W., Nie, L., Schauer, J. J., Yang, S., Xu, Y., and Zhang, Y.: Estimation of commercial cooking emissions in real-world operation: Particulate and gaseous emission factors, activity influencing and modelling, Environ. Pollut., 289, 117847, https://doi.org/10.1016/j.envpol.2021.117847, 2021.

Liu, J., Zhang, F., Xu, W., Chen, L., Ren, J., Jiang, S., Sun, Y., and Li, Z.: A large impact of cooking organic aerosol (COA) on particle hygroscopicity and CCN activity in urban atmosphere, J. Geophys. Res.-Atmos., 126, e2020JD033628, https://doi.org/10.1029/2020JD033628, 2021.

Liu, Z., Guan, D., Wei, W., Davis, S. J., Ciais, P., Bai, J., Peng, S., Zhang, Q., Hubacek, K., Marland, G., Andres, R. J., Crawford-Brown, D., Lin, J., Zhao, H., Hong, C., Boden, T. A., Feng, K., Peters, G. P., Xi, F., Liu, J., Li, Y., Zhao, Y., Zeng, N., and He, K.: Reduced carbon emission estimates from fossil fuel combustion and cement production in China, Nature, 524, 335–338, https://doi.org/10.1038/nature14677, 2015.

Lui, K. H., Bandowe, B. A. M., Ho, S. S. H., Chuang, H.-C., Cao, J.-J., Chuang, K.-J., Lee, S. C., Hu, D., and Ho, K. F.: Characterization of chemical components and bioreactivity of fine particulate matter ($PM_{2.5}$) during incense burning, Environ. Pollut., 213, 524–532, https://doi.org/10.1016/j.envpol.2016.02.053, 2016.

Martinsson, J., Eriksson, A. C., Nielsen, I. E., Malmborg, V. B., Ahlberg, E., Andersen, C., and Lindgren, R.: Impacts of combustion conditions and photochemical processing on the light absorption of biomass combustion aerosol, Environ. Sci. Technol., 49, 14663–14671, https://doi.org/10.1021/acs.est.5b03205, 2015.

McDuffie, E. E., Smith, S. J., O'Rourke, P., Tibrewal, K., Venkataraman, C., Marais, E. A., Zheng, B., Crippa, M., Brauer, M., and Martin, R. V.: A global anthropogenic emission inventory of atmospheric pollutants from sector- and fuel-specific sources (1970–2017): an application of the Community Emissions Data System (CEDS), Earth Syst. Sci. Data, 12, 3413–3442, https://doi.org/10.5194/essd-12-3413-2020, 2020.

Meng, W., Zhong, Q., Chen, Y., Shen, H., Yun, X., Smith, K. R., Li, B., Liu, J., Wang, X., Ma, J., Cheng, H., Zeng, E. Y., Guan, D., Russell, A. G., and Tao, S.: Energy and air pollution benefits of household fuel policies in northern China, P. Natl. Acad. Sci. USA, 116, 16773–16780, https://doi.org/10.1073/pnas.1904182116, 2019.

Ministry of Emergency Management of the PRC: Statistical data, https://www.mem.gov.cn/gk/tjsj/, last access: 8 September 2020.

National Bureau of Statistics: National data, https://data.stats.gov.cn/, last access: 2 December 2020.

National Institute for Nutrition and Health, Chinese Center for Disease Control and Prevention: Nutrition Data Yearbook, https://www.chinanutri.cn/, last access: 31 August 2021.

Pang, N., Gao, J., Zhao, P., Wang, Y., Xu, Z., and Chai, F.: The impact of fireworks control on air quality in four Northern Chinese cities during the Spring Festival, Atmos. Environ., 244, 117958, https://doi.org/10.1016/j.atmosenv.2020.117958, 2021.

Park, R. J., Kim, M. J., Jeong, J. I., Youn, D., and Kim, S.: A contribution of brown carbon aerosol to the aerosol light absorption and its radiative forcing in East Asia, Atmos. Environ., 44, 1414–1421, https://doi.org/10.1016/j.atmosenv.2010.01.042, 2010.

Peng, L., Zhang, Q., Yao, Z., Mauzerall, D. L., Kang, S., Du, Z., Zheng, Y., Xue, T., and He, K.: Underreported coal in statistics: A survey-based solid fuel consumption and emission inventory for the rural residential sector in China, Appl. Energy, 235, 1169–1182, https://doi.org/10.1016/j.apenergy.2018.11.043, 2019.

Que, D. E., Hou, W.-C., Lin, S.-L., Tsai, Y.-I., Lu, I.-C., Wang, L.-C., Young, L.-H., Yu, K.-L. J., Lai, C.-Y., Chao, H.-R., Hsu, Y.-C., Cui, K., Chen, S., Tayo, L. L., and Arcega, R. D.: Emission of carbonyl compounds from cooking oil fumes in the night market areas, Aerosol Air Qual. Res., 19, 1566–1578, https://doi.org/10.4209/aaqr.2019.06.0289, 2019.

Ramanathan, V. and Carmichael, G.: Global and regional climate changes due to black carbon, Nat. Geosci., 1, 221–227, https://doi.org/10.1038/ngeo156, 2008.

Saito, E., Tanaka, N., Miyazaki, A., and Tsuzaki, M.: Concentration and particle size distribution of polycyclic aromatic hydrocarbons formed by thermal cooking, Food Chem., 153, 285–291, https://doi.org/10.1016/j.foodchem.2013.12.055, 2014.

Saleh, R., Hennigan, C. J., McMeeking, G. R., Chuang, W. K., Robinson, E. S., Coe, H., Donahue, N. M., and Robinson, A. L.: Absorptivity of brown carbon in fresh and photo-chemically aged biomass-burning emissions, Atmos. Chem. Phys., 13, 7683–7693, https://doi.org/10.5194/acp-13-7683-2013, 2013.

See, S. W. and Balasubramanian, R.: Characterization of fine particle emissions from incense burning, Build. Environ., 46, 1074–1080, https://doi.org/10.1016/j.buildenv.2010.11.006, 2011.

Shen, G., Xue, M., Chen, Y., Yang, C., Li, W., Shen, H., Huang, Y., Zhang, Y., Chen, H., Zhu, Y., Wu, H., Ding, A., and Tao, S.: Comparison of carbonaceous particulate matter emission factors among different solid fuels burned in residential stoves, Atmos. Environ., 89, 337–345, https://doi.org/10.1016/j.atmosenv.2014.01.033, 2014.

Shen, H., Tsai, C.-M., Yuan, C.-S., Jen, Y.-H., and Ie, I.-R.: How incense and joss paper burning during the worship activities influences ambient mercury concentrations in indoor and outdoor environments of an Asian temple?, Chemosphere, 167, 530–540, https://doi.org/10.1016/j.chemosphere.2016.09.159, 2017.

Shi, Y., Zhang, N., Gao, J., Li, X., and Cai, Y.: Effect of fireworks display on perchlorate in air aerosols during the Spring Festival, Atmos. Environ., 45, 1323–1327, https://doi.org/10.1016/j.atmosenv.2010.11.056, 2011.

Sun, J., Zhi, G., Hitzenberger, R., Chen, Y., Tian, C., Zhang, Y., Feng, Y., Cheng, M., Zhang, Y., Cai, J., Chen, F., Qiu, Y., Jiang, Z., Li, J., Zhang, G., and Mo, Y.: Emission factors and light absorption properties of brown carbon from household coal combustion in China, Atmos. Chem. Phys., 17, 4769–4780, https://doi.org/10.5194/acp-17-4769-2017, 2017.

Sun, Y., He, Y., Kuang, Y., Xu, W., Song, S., Ma, N., Tao, J., Cheng, P., Wu, C., Su, H., Cheng, Y., Xie, C., Chen, C., Lei, L., Qiu, Y., Fu, P., Croteau, P., and Worsnop, D. R.: Chemical differences between PM_1 and $PM_{2.5}$ in highly polluted environment and implications in air pollution studies, Geophys. Res. Lett., 47, e2019GL086288, https://doi.org/10.1029/2019GL086288, 2020.

Sun, Y. L., Wang, Z. F., Fu, P. Q., Yang, T., Jiang, Q., Dong, H. B., Li, J., and Jia, J. J.: Aerosol composition, sources and processes during wintertime in Beijing, China, Atmos. Chem. Phys., 13, 4577–4592, https://doi.org/10.5194/acp-13-4577-2013, 2013.

Tanda, S., Licbinsky, R., Hegrova, J., and Goessler, W.: Impact of New Year's Eve fireworks on the size resolved element distributions in airborne particles, Environ. Int., 128, 371–378, https://doi.org/10.1016/j.envint.2019.04.071, 2019.

Tian, J., Wang, Q., Ni, H., Wang, M., Zhou, Y., Han, Y., Shen, Z., Pongpiachan, S., Zhang, N., Zhao, Z., Zhang, Q., Zhang, Y., Long, X., and Cao, J.: Emission characteristics of primary brown carbon absorption from biomass and coal burning: Development of an optical emission inventory for China, J. Geophys. Res.-Atmos., 124, 1879–1893, https://doi.org/10.1029/2018JD029352, 2019.

Tong, D., Cheng, J., Liu, Y., Yu, S., Yan, L., Hong, C., Qin, Y., Zhao, H., Zheng, Y., Geng, G., Li, M., Liu, F., Zhang, Y., Zheng, B., Clarke, L., and Zhang, Q.: Dynamic projection of anthropogenic emissions in China: methodology and 2015–2050 emission pathways under a range of socio-economic, climate policy, and pollution control scenarios, Atmos. Chem. Phys., 20, 5729–5757, https://doi.org/10.5194/acp-20-5729-2020, 2020.

Vecchi, R., Bernardoni, V., Cricchio, D., D'Alessandro, A., Fermo, P., Lucarelli, F., Nava, S., Piazzalunga, A., and Valli, G.: The impact of fireworks on airborne particles, Atmos. Environ., 42, 1121–1132, https://doi.org/10.1016/j.atmosenv.2007.10.047, 2008.

Venkataraman, C., Habib, G., Eiguren-Fernandez, A., Miguel, A. H., and Friedlander, S. K.: Residential biofuels in South Asia: Carbonaceous aerosol emissions and climate impacts, Science, 307, 1454–1456, https://doi.org/10.1126/science.1104359, 2005.

Wang, G., Cheng, S., Wei, W., Wen, W., Wang, X., and Yao, S.: Chemical characteristics of fine particles emitted from different Chinese cooking styles, Aerosol Air Qual. Res., 15, 2357–2366, https://doi.org/10.4209/aaqr.2015.02.0079, 2015.

Wang, H., Xiang, Z., Wang, L., Jing, S., Lou, S., Tao, S., Liu, J., Yu, M., Li, L., Lin, L., Chen, Y., Wiedensohler, A., and Chen, C.: Emissions of volatile organic compounds (VOCs) from cooking and their speciation: A case study for Shanghai with implications for China, Sci. Total Environ., 621, 1300–1309, https://doi.org/10.1016/j.scitotenv.2017.10.098, 2018.

Wang, L., Xiang, Z., Stevanovic, S., Ristovski, Z., Salimi, F., Gao, J., Wang, H., and Li, L.: Role of Chinese cooking emissions on ambient air quality and human health, Sci. Total Environ., 589, 173–181, https://doi.org/10.1016/j.scitotenv.2017.02.124, 2017.

Wang, L., Zheng, X., Stevanovic, S., Wu, X., Xiang, Z., Yu, M., and Liu, J.: Characterization particulate matter from several Chinese cooking dishes and implications in health effects, J. Environ. Sci., 72, 98–106, https://doi.org/10.1016/j.jes.2017.12.015, 2018.

Wang, Q., Sun, Y., Jiang, Q., Du, W., Sun, C., Fu, P., and Wang, Z.: Chemical composition of aerosol particles and light extinction apportionment before and during the heating season in Beijing, China, J. Geophys. Res.-Atmos., 120, 12708–12722, https://doi.org/10.1002/2015JD023871, 2015.

Wang, R., Tao, S., Wang, W., Liu, J., Shen, H., Shen, G., Wang, B., Liu, X., Li, W., Huang, Y., Zhang, Y., Lu, Y., Chen, H., Chen, Y., Wang, C., Zhu, D., Wang, X., Li, B., Liu, W., and Ma, J.: Black carbon emissions in China from 1949 to 2050, Environ. Sci. Technol., 46, 7595–7603, https://doi.org/10.1021/es3003684, 2012.

Wang, R., Tao, S., Shen, H., Huang, Y., Chen, H., Balkanski, Y., Boucher, O., Ciais, P., Shen, G., Li, W., Zhang, Y., Chen, Y., Lin, N., Su, S., Li, B., Liu, J., and Liu, W.: Trend in global black carbon emissions from 1960 to 2007, Environ. Sci. Technol., 48, 6780–6787, https://doi.org/10.1021/es5021422, 2014.

Wang, X., Heald, C. L., Ridley, D. A., Schwarz, J. P., Spackman, J. R., Perring, A. E., Coe, H., Liu, D., and Clarke, A. D.: Exploiting simultaneous observational constraints on mass and absorption to estimate the global direct radiative forcing of black carbon and brown carbon, Atmos. Chem. Phys., 14, 10989–11010, https://doi.org/10.5194/acp-14-10989-2014, 2014.

Wang, Y., Wang, Q., Ye, J., Li, L., Zhou, J., Ran, W., Zhang, R., Wu, Y., and Cao, J.: Chemical composition and sources of submicron aerosols in winter at a regional site in Beijing-Tianjin-Hebei region: Implications for the Joint Action Plan, Sci. Total Environ., 719, 137547, https://doi.org/10.1016/j.scitotenv.2020.137547, 2020.

Wei, J., Li, Z., Cribb, M., Huang, W., Xue, W., Sun, L., Guo, J., Peng, Y., Li, J., Lyapustin, A., Liu, L., Wu, H., and Song, Y.: Improved 1 km resolution $PM_{2.5}$ estimates across China using enhanced space–time extremely randomized trees, Atmos. Chem. Phys., 20, 3273–3289, https://doi.org/10.5194/acp-20-3273-2020, 2020.

Wei, J., Li, Z., Lyapustin, A., Sun, L., Peng, Y., Xue, W., Su, T., and Cribb, M.: Reconstructing 1-km-resolution high-quality $PM_{2.5}$ data records from 2000 to 2018 in China: Spatiotemporal variations and policy implications, Remote Sens. Environ., 252, 112136, https://doi.org/10.1016/j.rse.2020.112136, 2021.

WorldPop and Center for International Earth Science Information Network (CIESIN): Global High Resolution Population Denominators Project, Funded by The Bill and Melinda Gates Foundation (OPP1134076), https://doi.org/10.5258/SOTON/WP00674, 2018.

Wu, C., Bao, L., Guo, Y., Li, S., and Zeng, E. Y.: Barbecue fumes: An overlooked source of health hazards in outdoor settings, Environ. Sci. Technol., 49, 10607–10615, https://doi.org/10.1021/acs.est.5b01494, 2015.

Wu, J., Kong, S., Wu, F., Cheng, Y., Zheng, S., Yan, Q., Zheng, H., Yang, G., Zheng, M., Liu, D., Zhao, D., and Qi, S.: Estimating the open biomass burning emissions in central and eastern China from 2003 to 2015 based on satellite observation, Atmos. Chem. Phys., 18, 11623–11646, https://doi.org/10.5194/acp-18-11623-2018, 2018.

Wu, J., Kong, S., Wu, F., Cheng, Y., Zheng, S., Qin, S., Liu, X., Yan, Q., Zheng, H., Zheng, M., Yan, Y., Liu, D., Ding, S., Zhao, D., Shen, G., Zhao, T., and Qi, S.: The moving of high emission for biomass burning in China: View from multi-year emission estimation and human-driven forces, Environ. Int., 142, 105812, https://doi.org/10.1016/j.envint.2020.105812, 2020.

Wu, J., Kong, S., Zeng, X., Cheng, Y., Yan, Q., Zheng, H., Yan, Y., Zheng, S., Liu, D., Zhang, X., Fu, P., Wang, S., and Qi, S.: First high-resolution emission inventory of levoglucosan for biomass burning and non-biomass burning sources in China, Environ. Sci. Technol., 55, 1497–1507, https://doi.org/10.1021/acs.est.0c06675, 2021.

Xiang, Z., Wang, H., Stevanovic, S., Jing, S., Lou, S., Tao, S., Li, L., Liu, J., Yu, M., and Wang, L.: Assessing impacts of factors on carbonyl compounds emissions produced from several typical Chinese cooking, Build. Environ., 125, 348–355, https://doi.org/10.1016/j.buildenv.2017.08.045, 2017.

Xu M., Chao X., Zhang B., Liu S., Yin J., and Gan S.: Study on the investigation, analysis and countermeasures for the current status of mutton sheep industry in Xinjiang (In Chinese), Acta Ecologiae Animalis Domastici, 39, 85–89, 2018.

Yan, Q., Kong, S., Yan, Y., Liu, H., Wang, W., Chen, K., Yin, Y., Zheng, H., Wu, J., Yao, L., Zeng, X., Cheng, Y., Zheng, S., Wu, F., Niu, Z., Zhang, Y., Zheng, M., Zhao, D., Liu, D., and Qi, S.: Emission and simulation of primary fine and submicron particles and water-soluble ions from domestic coal combustion in China, Atmos. Environ., 224, 117308, https://doi.org/10.1016/j.atmosenv.2020.117308, 2020.

Yang, C.-R., Ko, T.-H., Lin, Y.-C., Lee, S.-Z., Chang, Y.-F., and Hsueh, H.-T.: Oyster shell reduces PAHs and particulate matter from incense burning, Environ. Chem. Lett., 11, 33–40, https://doi.org/10.1007/s10311-012-0374-2, 2013.

Yang, H.-H., Jung, R.-C., Wang, Y.-F., and Hsieh, L.-T.: Polycyclic aromatic hydrocarbon emissions from joss paper furnaces, Atmos. Environ., 39, 3305–3312, https://doi.org/10.1016/j.atmosenv.2005.01.052, 2005.

Yao, L., Wang, D., Fu, Q., Qiao, L., Wang, H., Li, L., Sun, W., Li, Q., Wang, L., Yang, X., Zhao, Z., Kan, H., Xian, A., Wang, G., Xiao, H., and Chen, J.: The effects of firework regulation on air quality and public health during the Chinese Spring Festival from 2013 to 2017 in a Chinese megacity, Environ. Int., 126, 96–106, https://doi.org/10.1016/j.envint.2019.01.037, 2019.

Zhang, A., Wang, Y., Zhang, Y., Weber, R. J., Song, Y., Ke, Z., and Zou, Y.: Modeling the global radiative effect of brown carbon: a potentially larger heating source in the tropical free troposphere than black carbon, Atmos. Chem. Phys., 20, 1901–1920, https://doi.org/10.5194/acp-20-1901-2020, 2020.

Zhang, L., Gao, Y., Wu, S., Zhang, S., Smith, K. R., Yao, X., and Gao, H.: Global impact of atmospheric arsenic on health risk: 2005 to 2015, P. Natl. Acad. Sci. USA, 117, 13975–13982, https://doi.org/10.1073/pnas.2002580117, 2020a.

Zhang, L., Luo, Z., Du, W., Li, G., Shen, G., Cheng, H., and Tao, S.: Light absorption properties and absorption emission factors for indoor biomass burning, Environ. Pollut., 267, 115652, https://doi.org/10.1016/j.envpol.2020.115652, 2020b.

Zhang, L., Luo, Z., Li, Y., Chen, Y., Du, W., Li, G., Cheng, H., Shen, G., and Tao, S.: Optically measured black and particulate brown carbon emission factors from real-world residential combustion predominantly affected by fuel differences, Environ. Sci. Technol., 55, 169–178, https://doi.org/10.1021/acs.est.0c04784, 2021.

Zhang, Q., Zheng, Y., Tong, D., Shao, M., Wang, S., Zhang, Y., Xu, X., Wang, J., He, H., Liu, W., Ding, Y., Lei, Y., Li, J., Wang, Z., Zhang, X., Wang, Y., Cheng, J., Liu, Y., Shi, Q., Yan, L., Geng, G., Hong, C., Li, M., Liu, F., Zheng, B., Cao, J., Ding, A., Gao, J., Fu, Q., Huo, J., Liu, B., Liu, Z., Yang, F., He, K., and Hao, J.: Drivers of improved $PM_{2.5}$ air quality in China from 2013 to 2017, P. Natl. Acad. Sci. USA, 116, 24463–24469, https://doi.org/10.1073/pnas.1907956116, 2019.

Zhang, S., Zhong, L., Chen, X., Liu, Y., Zhai, X., Xue, Y., Wang, W., Liu, J., and Xu, K.: Emissions characteristics of hazardous air pollutants from the incineration of sacrificial offerings, Atmosphere, 10, 332, https://doi.org/10.3390/atmos10060332, 2019.

Zhang, Y., Kong, S., Sheng, J., Zhao, D., Ding, D., Yao, L., Zheng, H., Wu, J., Cheng, Y., Yan, Q., Niu, Z., Zheng, S., Wu, F., Yan, Y., Liu, D., and Qi, S.: Real-time emission and stage-dependent emission factors/ratios of specific volatile organic compounds from residential biomass combustion in China, Atmos. Res., 248, 105189, https://doi.org/10.1016/j.atmosres.2020.105189, 2021.

Zhang, Z., Zhu, W., Hu, M., Liu, K., Wang, H., Tang, R., Shen, R., Yu, Y., Tan, R., Song, K., Li, Y., Zhang, W., Zhang, Z., Xu, H., Shuai, S., Li, S., Chen, Y., Li, J., Wang, Y., and Guo, S.: Formation and evolution of secondary organic aerosols derived from urban-lifestyle sources: vehicle exhaust and cooking emissions, Atmos. Chem. Phys., 21, 15221–15237, https://doi.org/10.5194/acp-21-15221-2021, 2021.

Zhao, Y., Chen, C., and Zhao, B.: Is oil temperature a key factor influencing air pollutant emissions from Chinese cooking?, Atmos. Environ., 193, 190–197, https://doi.org/10.1016/j.atmosenv.2018.09.012, 2018.

Zhao, Y., Chen, C., and Zhao, B.: Emission characteristics of $PM_{2.5}$-bound chemicals from residential Chinese cooking, Build. Environ., 149, 623–629, https://doi.org/10.1016/j.buildenv.2018.12.060, 2019.

Zheng, B., Tong, D., Li, M., Liu, F., Hong, C., Geng, G., Li, H., Li, X., Peng, L., Qi, J., Yan, L., Zhang, Y., Zhao, H., Zheng, Y., He, K., and Zhang, Q.: Trends in China's anthropogenic emissions since 2010 as the consequence of clean air actions, Atmos. Chem. Phys., 18, 14095–14111, https://doi.org/10.5194/acp-18-14095-2018, 2018.

Zhong, Q., Shen, H., Yun, X., Chen, Y., Ren, Y., Xu, H., Shen, G., Du, W., Meng, J., Li, W., Ma, J., and Tao, S.: Global Sulfur Dioxide Emissions and the Driving Forces, Environ. Sci. Technol., 54, 65086517, https://doi.org/10.1021/acs.est.9b07696, 2020.

Zhu, W., Guo, S., Zhang, Z., Wang, H., Yu, Y., Chen, Z., Shen, R., Tan, R., Song, K., Liu, K., Tang, R., Liu, Y., Lou, S., Li, Y., Zhang, W., Zhang, Z., Shuai, S., Xu, H., Li, S., Chen, Y., Hu, M., Canonaco, F., and Prévôt, A. S. H.: Mass spectral characterization of secondary organic aerosol from urban cooking and vehicular sources, Atmos. Chem. Phys., 21, 15065–15079, https://doi.org/10.5194/acp-21-15065-2021, 2021a.

Zhu, W., Zhou, M., Cheng, Z., Yan, N., Huang, C., Qiao, L., Wang, H., Liu, Y., Lou, S., and Guo, S.: Seasonal variation of aerosol compositions in Shanghai, China: Insights from particle aerosol mass spectrometer observations, Sci. Total Environ., 771, 144948, https://doi.org/10.1016/j.scitotenv.2021.144948, 2021b.

Zotter, P., Herich, H., Gysel, M., El-Haddad, I., Zhang, Y., Močnik, G., Hüglin, C., Baltensperger, U., Szidat, S., and Prévôt, A. S. H.: Evaluation of the absorption Ångström exponents for traffic and wood burning in the Aethalometer-based source apportionment using radiocarbon measurements of ambient aerosol, Atmos. Chem. Phys., 17, 4229–4249, https://doi.org/10.5194/acp-17-4229-2017, 2017.